Master of Science Thesis
VT2018

Evaluation of Tomodirect for treatment of thoracic and abdominal cases

Sara Talozi

Supervisors

Kristoffer Petersson and Per Engström, Lund

Department of Medical Radiation Physics,
Clinical Sciences, Lund
Lund University
www.msf.lu.se

Swedish popular summary (Populärvetenskaplig sammanfattning)

Kan TomoDirect vara ett bättre alternativ för behandling av cancer i thorax och bukområdet?

Sedan 1970-talet har antalet rapporterade cancerfall dubblerats, dels på grund av förändrade levnadsvanor och dels på grund av bättre screeningmetoder som upptäcker cancern i tidigt skede. Tidig upptäckt av cancern i kombination med utvecklad cancerbehandling har bidragit till att risken för att avlida av cancer har minskat. Cancerbehandling sker huvudsakligen genom operation, strålbehandling eller med cellgifter, eller en kombination av dessa. Varannan cancersjuk patient får under sin behandlingstid någon form av strålbehandling. Det kan vara antingen för att bota cancern, minska risken för återfall eller lindra sjukdomen.

Joniserande strålning används inom strålbehandling för att skada tumörcellernas arvsmassa (DNA). De två vanligaste metoderna som används för strålbehandling är extern och intern strålbehandling. Vid extern strålbehandling används en extern källa som placeras utanför patienten och joniserande strålning levereras i form av en stråle till tumören. Vid intern strålterapi förs en strålkälla lika litet som ett frö in i kroppen så nära tumören som möjligt.

Målet med en effektiv strålbehandling är att den joniserande strålningen endast träffar tumören och frisk vävnad skonas så mycket som möjlig. Dock kan bland annat osäkerheter inom strålbehandlingen såsom inkorrekt patientpositionering, tumörförändringar och andningsrörelser leda till att stråldosen blir utsmetad/blurrad, vilket kan leda till att en del av strålningen träffar den friska vävnaden som vi vill skona istället för tumören. Detta kan förklaras med hjälp av en jämförelse till ett fotografi av en person som rör sig, vid exponering under rörelse resulterar detta i att bilden blir utsmetad. På liknande sätt kan en patient som rör sig eller som dess inre organ rör sig under behandling, resultera i en utsmetad/blurrad stråldos. Blurrning av stråldosen tar man vanligtvis hänsyn till genom att öka marginalerna för behandlingsområdet. Men det kan även förkomma inbördes rörelser mellan bestrålningsmaskinens delar och tumören (s.k interplay effekter) som leder till ojämn strålning kring tumören. Dessa effekter kan man inte alltid kompensera för med hjälp av utökning av behandlingsmarginaler då de är mer komplicerade och beror oftast på många olika behandlingsparametrar. Interplay effekter och blurrning är oftast ett problem i thorax och bukområdet, där andningsrörelser leder till tumörrörelser och andra anatomiska rörelser.

Patienter med cancer i thorax och bukområdet behandlas idag med så kallad konventionell teknik eller rotations-behandlingsteknik (exempelvis TomoHelical). För den konventionella tekniken används strålfält med uniform intensitet och patientbritsen är fast under behandlingen. Fördelen med denna teknik är att strålbehandlingen generellt sett går fort. Nackdelen med den konventionella tekniken är att en del strålning träffar frisk vävnad på grund av att man ofta utökar behandlingsmarginalen för att kompensera för eventuella rörelser av organ och därmed används bredare strålfält med uniform intensitet för att täcka behandlingsområdet. Den andra nackdelen är användningen av få strålfält, vilket är ett problem då målet är att tumören ska erhålla hög stråldos och därför måste dessa fält ha väldigt

hög intensitet. Dock är det inte enbart tumören i detta fall som får hög stråldos, men även omkringliggande frisk vävnad som träffas av dessa strålfält.

Som tidigare nämnts används idag även TomoHelical som är en tomoterapiteknik och är en speciell form av strålbehandlingsteknik. TomoHelical är en teknik där maskinen roterar runt patienten och levererar strålning medan patientbritsen rör sig kontinuerligt. Detta medför att en del strålning med låg intensitet träffar frisk vävnad. Det är ett problem som kan öka vid andningsrörelser, eftersom en större mängd låg-intensitets strålning kan träffa frisk vävnad istället för tumören.

Tomoterapisystemet erbjuder även en annan teknik så kallad TomoDirect där endast ett fåtal vinklar används (mellan 2–12 vinklar) vid bestrålning medan patientbritsen rör sig. Denna teknik används runt omkring i världen för det mesta till bröstbestrålning. TomoDirect skulle kunna vara ett alternativ till behandling med konventionell teknik i thorax och bukområdet där vi har andningsrörelser, och man bland annat vill undvika bestrålning med stora fält med uniform intensitet. Istället används fält med varierande intensitet. I och med att intensiteten på dessa fält varierar är det möjligt att det bidrar till lägre stråldos till frisk vävnad, vilket är fördelaktigt jämfört med den konventionella tekniken. TomoDirect kan även vara fördelaktigt för patienter med cancer i thorax och bukområdet som behandlas idag med TomoHelical eftersom strålningen levereras med fasta vinklar och en lägre mängd låg-intensitets strålning träffar frisk vävnad.

I detta examensarbete presenteras en separat jämförelse mellan TomoDirect och TomoHelical, och TomoDirect och konventionell teknik för att undersöka om TomoDirect är ett bättre alternativ för cancerbehandling i thorax och bukområdet.

Abstract

Aim: The tomotherapy system offers two radiation techniques, TomoHelical (TH) and TomoDirect (TD). The aim of this master thesis was to evaluate TD as a treatment alternative mainly by comparing TD treatment plans with 3DCRT plans and comparing TD plans with TH plans, separately, in the thoracic and abdominal regions. An additional aim was to examine if the current patient specific quality control (QC) is sufficient for TD treatments.

Material & Methods: Computed tomography (CT) scans of 20 patients with different diagnosis who received radiotherapy in the thoracic or abdominal region were used. The patients were randomly selected. TD plans were created in Tomotherapy planning system version 5.1.1.6. TD plans were compared with TH and 3DCRT plans regarding the planning target volume (PTV) coverage, homogeneity index (HI), conformity index (CI), mean absorbed dose to organs at risk (OAR) and beam-on time. The Delta^4 phantom+ was used for QC of the treatment plans. To get an insight of the robustness of TD, Hexamotion was used in conjunction with the Delta^4 phantom+ for motion simulation.

Results: The plan comparison between TD and TH for the thoracic cases showed equal PTV coverage, mean absorbed dose to OAR, HI and beam-on time. TH showed better CI than TD ($p=0.02$). For abdominal cases, the mean absorbed dose to OAR and CI were comparable between TD and TH. Compared to TH, TD plans had shorter beam-on time in the abdominal region (TD: 2.4-5.4 min, TH: 4.1-8.6 min) whereas TH provided better homogeneity ($p=0.04$). TD plans showed significantly better PTV coverage than 3DCRT both for the thoracic and abdominal cases ($p=0.01$). For the thoracic cases, CI, HI and beam-on times were equal in TD and 3DCRT plans whereas the beam-on time was longer for TD plans ($p=0.01$). The mean absorbed dose to the right lung (contralateral for 4 of 5 cases) and heart were equal between TD and 3DCRT plans. TD reduced the mean absorbed dose to left lung (ipsilateral lung for 4 of 5 cases) ($p=0.01$). For the abdominal cases, CI, HI, mean absorbed dose to OAR and the beam-on times were equal. The QC measurements of the treatment plans were all clinically acceptable. Regardless of the used technique, the motion simulation measurements showed that the tomotherapy system is robust for +5 mm motion in cranio-caudal direction.

Summary and conclusions: According to the comparison study of using TD in the thoracic and abdominal region, the benefits of TD relative to TH were beam-on time reduction for some cases (abdominal cases) and a reduced low dose volume. Compared to 3DCRT, TD provided an excellent PTV coverage. The present QC method (Delta^4 phantom+) is suitable for measuring TD plans with ≥ 3 beam angles. Further research using simulated motion could bring more clarity about TD robustness in the thoracic and abdominal region

Table of contents

Abbreviations

3DCRT	Three-dimensional conformal radiotherapy
CI	Conformity index
CT	Computed tomography
CTV	Clinical target volume
DQA	Delivery quality assurance
DVH	Dose-volume histogram
H_0	Null hypothesis
H_1	Alternative hypothesis
HI	Homogeneity index
IMRT	Intensity modulated radiotherapy
kVCT	Kilovoltage CT
MLC	Multi leaf collimator
MVCT	Megavoltage CT
OAR	Organs at risk
PRV	Planning organ at risk volume
PTV	Planning target volume
SAD	Source axis distance
TD	TomoDirect
TH	TomoHelical
QC	Quality control

1. Introduction

In Sweden, more than 60 000 people were diagnosed with cancer in year 2015. This is about twice as many as were diagnosed yearly in the 1970's, which is mainly due to older population, different life style and better screening methods to detect cancer. More than one fifth of these 60 000 people were diagnosed with thoracic cancer, which is cancer in the breast, lung and chest region (1). Cancer is mainly treated with surgery, radiotherapy or chemotherapy. Often, a combination of these methods is used, for example irradiation after surgery to kill the remaining cancer cells (1).

In radiotherapy, ionizing radiation is used to damage the DNA of the tumor cells. There are mainly two types of radiotherapy: internal (Brachytherapy) which involves radiation sources that are placed inside or close to the region to be treated and external radiotherapy, in which external radiation beams are used. In external radiotherapy, radiation beams coming from several directions pass through the patient, which kills both cancerous and healthy cells. The radiation beams in external radiotherapy are often delivered by a linear accelerator. A linear accelerator is a machine that accelerate charged particles (e.g. electrons) to very high velocities, for electrons close to the speed of light. The charged particles can be used directly to treat the tumor but often a heavy metal is placed in the path of the accelerated electrons and when they collide, high energy X-rays (Bremsstrahlung and photons) are produced. These X-rays are then used for the radiotherapy treatment. To ensure that the radiation beam is delivered to the target volume (tumor), a treatment plan is needed. Different techniques can be used for the creation and delivery of the treatment plans such as three-dimensional conformal radiotherapy (3DCRT) and intensity modulated radiotherapy (IMRT), but the aim is the same to deliver high dose to the tumor while minimizing the dose to normal tissue. In 3DCRT, beams with uniform intensity are generally used to deliver radiation, in contrast to IMRT which generally uses non-uniform beams modulated by a computer controlled multi leaf collimator (MLC).

An ideal scenario for efficient radiotherapy is to deliver sufficient radiation to the tumor while avoiding excessive radiation dose to surrounding healthy tissue. Geometric uncertainties in radiotherapy must be reduced to achieve this ideal scenario. Examples of uncertainties are: set-up error due to incorrect patient positioning, tumor deformation and lung and cardiac motion during normal breathing (2). The effect of motion and random setup errors leads to a blurry dose distribution, which leads to a less conformal dose distribution. Blurring can occur both for intra-fractional movements (i.e. the delivered dose will be blurred in every treatment session) and interfractional motion (motion between the treatment sessions). With interfractional motion, the daily dose distribution will be sharp but the total dose distribution after all treatment sessions will be blurred. In this thesis, focus will be on radiotherapy planning in the thoracic and abdominal regions, where lung and cardiac motion during normal breathing causes uncertainties in tumor position. To avoid under-dosage of the tumor, different techniques can be used, e.g. gated treatment or tumor tracking. The most common way to handle the motion for 3DCRT treatment plans is to extend the treatment margin, i.e. you treat the entire region in which the tumor moves. However, this results in larger volumes of normal tissue being treated. For IMRT, the simultaneous movement of the treatment delivery (for example MLC movement) and the tumor, cause interplay effects which results in unwanted heterogeneous dose distribution. These effects are difficult to predict and cannot be handled only by extending the treatment margin (2).

Skånes university hospital provides a specific radiotherapy technique since 2009, called tomotherapy. The TomoTherapy HD system is an intensity modulated radiation therapy

system with a linear accelerator mounted on a ring-shaped gantry. The system can deliver radiation in 360° with the patient moving through the gantry with a continuous couch movement. This helical delivery enables a homogeneous radiation dose to be delivered to the target volume. This modality is called TomoHelical (TH). The tomotherapy machine can also deliver radiation in discrete beam angles, which is called TomoDirect (TD). This technique is not utilized in the clinic for treatment of thoracic and abdominal cancer. Thus, exploring TD as treatment alternative for radiotherapy in these regions will be the focus of this thesis. TD uses intensity modulated radiation beams which can be advantageous compared to 3DCRT in terms of minimize the radiation dose to healthy tissue and better dose coverage of the treatment volume. The use of discrete beam angles in TD can be useful for the patients with thoracic and abdominal cancer that today receives treatment with TH, to minimize the low intensity radiation dose to healthy tissue.

To verify that the treatment machine is able to deliver the patient treatment plan as intended, a patient specific quality control (QC) must be performed. The patient specific QC method varies for the different type of treatment techniques. An implementation of a new treatment technique such as TD requires an investigation of new as well as current QC methods (3). The present QC method used in the clinic entails the use of a Delta^4 phantom+ to measure TH treatment plans. An evaluation of the present QC method utilized for TD should disclose possible problems with the method, which would function as a basis for further investigation of new QC methods for TD.

2. Aim

The aim of this master thesis was to evaluate TD as a treatment alternative mainly by comparing TD treatment plans with 3DCRT plans and comparing TD plans with TH plans, separately, in the thoracic and abdominal regions. The results from this study should indicate if these patient groups should be prioritized for treatment with TD.

An additional aim was to examine if the current patient specific QC method is sufficient for TD treatments or if there is a need for another QC method, and what features this QC method should have.

Questions to be answered:

- What are the benefits of TD compared to 3DCRT and TH?
- Is the current patient specific QC method in the clinic sufficient for TD?

3. Theoretical background

3.1. 3D conformal radiation therapy

The basic idea of delivering high dose to the tumor while minimizing the dose to normal tissue has been known for many decades. For example, the use of tangential fields for breast cancer treatment to reduce lung doses due to the risk of fibrosis of the lung was reported already in 1925. However, the use of 3DCRT was not possible until the clinical introduction of the computed tomography (CT) scanner in the early 1970s. The development of the CT scanner allowed for the first time acquisition of full anatomical information in three dimensions, for an individual patient. This information makes 3D treatment planning possible thanks to the electron density information received from the CT scan. Beam directions are chosen by the treatment planner and beam apertures are shaped based on the planning target volume (PTV) in a beams eye-view. This is utilized to get a conformal dose distribution, i.e. a high dose to the target volume and a quick dose fall-off outside this volume (4). To achieve that, an MLC is used. The MLC is a collimator with moveable leaves, which is used to block the radiation beam. Each MLC leaf is optimized to shape the field around the target volume which minimize the dose to normal tissue (4).

3.2. Intensity-modulated radiation therapy

IMRT is a conformal radiotherapy technique which aim is to deliver the radiation dose precisely to the tumor and avoiding high dose to organs at risk (OAR), such as 3DCRT. The IMRT technique allows the user to modulate the intensity of each radiation beam to control the dose distribution to target, unlike the 3DCRT which uses beams with uniform intensity. A conformal dose distribution to target and low dose to OAR are achieved by using several beams. In contrast to 3DCRT, for which forward planning (the planner chooses the beams and dose information is obtained afterwards) is used and the resulting treatment plan is depending on the planner's skills, an IMRT treatment planning software (optimizer) is used for the IMRT technique to find the best plan based on the specified dose limits for tumor and OAR (5).

The two most common techniques to deliver IMRT are segmental IMRT and dynamic IMRT. With segmental IMRT, several MLC segments (beam openings) are created for each beam orientation. The field intensity is modulated by controlling the size, shape and opening time of the different segments. With dynamic IMRT technique, the dose delivery is not halted between the reshape of each segment but take into account the motion between shapes for a more time efficient delivery. The speed variation of the leaves and the distance between them, modulate the intensity of the radiation (5).

3.3. Tomotherapy

The concept of tomotherapy was to treat patients with a fan beam slice by slice. This gives the modality its name from the greek word tomo, which means slice. The TomoTherapy HD system (TomoTherapy Inc, Madison,WI, USA) is an IMRT system with a linear accelerator mounted on a rotating gantry ring. The MLC has leaves which are either open or closed and can shift between these states quickly to modulate the intensity of the rotating fan beam. The couch moves continually during the treatment through the gantry while the radiation is delivered (6). A 3,5 Megavoltage CT-scan (MVCT) of patient anatomy can be obtained for

verification of patient position to ensure that the planned dose will be delivered precisely to the target volume (7). The tomotherapy system offers two radiation techniques, TH and TD.

3.3.1. TomoHelical

TH is a technique where the gantry rotates and delivers radiation from all (360°) angles while the patient couch is moving through the beam. During the treatment procedure the MLC leaves are moving to modulate the field. With TH there is an opportunity to deliver narrow beamlets which are optimized to the tumor target. This method provides a conformal dose distribution and minimize the dose to OAR due to dose fall-off outside the target (8). It has been reported in multiple studies that the helical technique as other rotational techniques cause a large dose bath, which means that surrounding normal tissue receive a low radiation dose (9) (10) (11). This is a disadvantage of the TH technique, as with all rotational radiotherapy techniques, because the dose bath can be a risk for radiation induced cancer, and other acute and late adverse effects. In contrast, TH enables a more homogenous radiation dose to be delivered to the tumor and more conformal dose distribution than TD.

3.3.2. TomoDirect

Unlike the helical technique, TD is a technique where the radiation is delivered in discrete angles while the gantry is fixed. The couch is moving the patient through the beam while the radiation is delivered in a certain angle, and back out again when the beam is delivered. In order to deliver the next beam, the gantry rotates to the selected angle and the process is repeated. The number of times this process is repeated depends on the number of angles that is used (12). The maximum number of beam angles that can be used is twelve. A high number of beam angles results in longer treatment times but also usually better treatment due to increased modulation capabilities compared to the use of few beam angles. In comparison with TH, the direct mode generally provides a decrease in treatment time (12) and may decrease dose to normal tissue (13) because the dose bath may decrease.

3.3.3. System overview

A 6 MV linear accelerator mounted on a gantry ring is used to generate a radiation beam (Figure 1). The jaws are used to shape the beam into either a 1.0, 2.5, or 5 cm wide fan beam in superior-inferior (y-direction) with an extension of 40 cm in lateral direction (x-direction) at isocenter. The binary MLC is used to modulate the beam. On the gantry ring, in the opposite side of the linear accelerator, a detector system is mounted to collect data, mainly for MVCT image acquisition. The source to detector distance is 145 cm, and the source axis distance (SAD) is 85 cm (14).

A major difference between the design of the tomotherapy system and other linear accelerators, besides the ring gantry design, is the lack of flattening filter. A flattening filter free system can deliver radiation with a higher dose rate than a system with a flattening filter. A higher dose rate decreases the dose delivery time, which is an advantage in e.g. the thorax region due to interplay effects (2) and it is more comfortable for the patients.

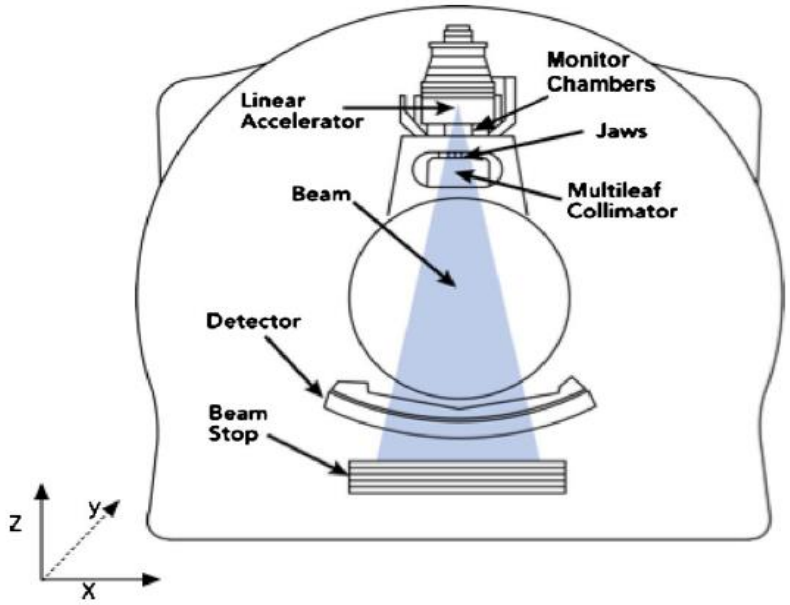

Figure 1. An overview of the tomotherapy machine illustrating the linear accelerator, the detector system, and the multileaf collimator (14).

The MLC consist of 64 leaves, which can either be fully closed or fully open. The emitted radiation of a single open MLC leaf is defined as the beamlet. The size of each beamlet is 0.625 cm at isocenter. Moreover, each rotation is divided into 51 projections, and each projection has a unique opening time for each MLC leaf, allowing for the beam modulation.

Different parameters can be adjusted to modulate the projection. One of these parameters is the modulation factor. The definition of the modulation factor is maximum leaf open time divided with the average leaf open time for a projection. A modulation factor of one means that all beamlets have equal intensity. The second parameter is pitch. The pitch has two definitions depending on the used technique, TH or TD. In TH, the definition of the pitch is couch traveling per gantry rotation in the units of field width. The pitch determines the degree of overlap between adjacent rotation (15). In TD, the pitch is defined as the distance the couch travel per MLC segment (16).

3.4. Quality Assurance

To ensure that the treatment machine is able to deliver the treatment plan as intended, a patient specific QC must be performed. The process of recalculating treatment plans on a phantom geometry and controlling the delivery through dose measurements is called DQA (delivery quality assurance). A CT scan of the phantom is imported to the tomotherapy planning system to perform the DQA. The plan is then recalculated on the phantom CT-scan (14). The comparison between calculated dose distributions and the measured ones are performed with the use of the Delta^4 phantom+ (Scandidos, Uppsala, Sweden). To evaluate difference between measured and calculated dose distribution, the gamma pass evaluation is used, see Appendix A.

3.4.1. Delta^4 phantom+

The Delta^4 phantom+ consists of 1069 p-type cylindrical Silicon diodes arranged in two orthogonal planes (horizontal and vertical) and placed in a 40 cm long cylindrical polymethylmethacrylate (PMMA) phantom. In the central area (6 cm × 6 cm), the diodes are spaced at 5 mm intervals, and outside this area, at 10 mm intervals. The two orthogonal detector planes (Figure 2) provides measurement in the isocentric target region (17).

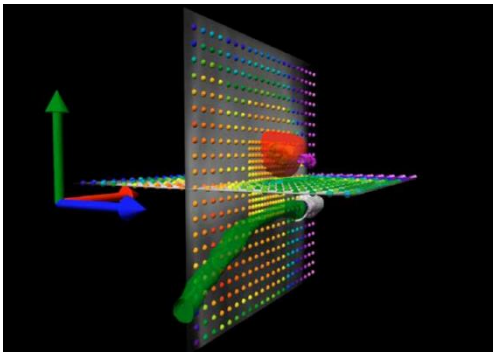

Figure 2. Detector arrangements (17).

The Delta^4 device (Figure 3) record measured dose by using the radiation pulse delivered by the tomotherapy machine. As the radiation pulse is detected by the diode, the electrometer changes from pulse searching mode to measurement mode. This mode remains until the next pulse arrives and if no pulse is coming the system reverts to the search mode. There is no beam geometry information to the Delta^4 from the tomotherapy which cause that no volumetric dose interpolation can be done, and the dose distribution is only evaluated in the two orthogonal measurement planes (18).

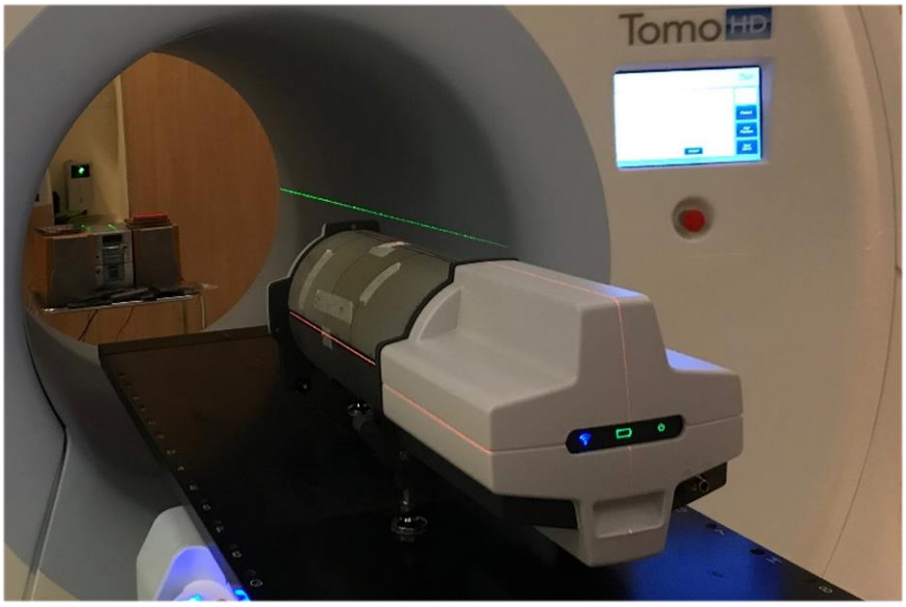

Figure 3. The Delta^4 phantom+ positioned for DQA measurements at the tomotherapy system.

3.5. Conformity and homogeneity index

3.5.1 Radiation conformity index

The radiation conformity index (CI) has been defined by Knöös T et al. (1998) as following (19):

$$CI = \frac{V_{\mathrm{PTV}}}{V_i}, \qquad \textit{Eq. 1}$$

where V_{PTV} is the PTV volume and V_i is the volume receiving 95% of the prescribed dose. The conformity index is used for determining the degree of conformity of a dose distribution. An ideal CI is equal to one, which corresponds to a high conformity or perfect dose coverage. A CI larger than one, could indicate that the PTV volume is not entirely covered by the 95% isodose.

3.5.2 Homogeneity index

The homogeneity index (HI) is a tool used for evaluating the homogeneity of the planned and/ or delivered dose distribution in the target volume. The homogeneity index is defined as following (20):

$$HI = \frac{D_{2\%} - D_{98\%}}{D_{\mathrm{Prescription}}}, \qquad \textit{Eq. 2}$$

where $D_{2\%}$ is the absorbed dose that 2% of the PTV receives, $D_{98\%}$ is the absorbed dose that 98% of the PTV receives and $D_{\mathrm{Prescription}}$ is the dose prescribed to the PTV. A low HI corresponds to a more homogenous dose distribution within the target volume compared to a large HI.

3.6. Statistical test

3.6.1. Sign test

The sign test is a non-parametric test and devised for paired data that are not normally distributed. Only information about the sign (+ or -) of a difference is used in the sign test. For example, if there is a comparison between two treatments, A and B, the null hypothesis (H_0) would be that there is no difference between A and B. An alternative hypothesis (H_1) for a one-sided test, would be that treatment A is better than B. For every compared pair, the sign + or - is given depending on if treatment A is superior respectively inferior to treatment B. In the cases when A and B are equal, the sign is ignored (21).

The p-value of the sign test is given by the binomial distribution in Eq. 3:

$$p = \sum_{i=0}^{k} \frac{N!}{i!\,(N-i)} \cdot q^i \cdot (1-q)^{N-i} \qquad \textit{Eq. 3}$$

where N=n^++n^-, n^+ is the number of times the sign + is given, n^- is the number of times the sign - is given, k is the smallest value of n^+ and n^- and q is equal to 0.5 which is the random probability. H_0 can be rejected if the p-value is below a chosen significance level α, and H_1 can be assumed (22).

4. Materials and methods

4.1. Materials

CT scans of 20 patients who received radiotherapy in the thoracic or abdominal region were used. Ten patients received radiotherapy with 3DCRT technique and ten patients with TH technique. The 3DCRT and TH treatment plans were performed by experienced treatment planners. The patients were randomly selected from the statistic file for treatment plans between 2014-2018 of patients with thoracic and abdominal cancer in the radiotherapy building at Skåne university hospital. TD plans were created in Tomotherapy planning system version 5.1.1.6 by the author of this thesis (medical physics student) with supervision of an experienced physicist. Patient characteristics can be seen in Table 1 for the thoracic cases and Table 2 for the abdominal cases.

Table 1. Age, gender, diagnose, target location and side, total radiation dose, number of radiotherapy fractions and treatment technique for the thoracic cases.

Case number	Age	Gender	Diagnose	Target location	Target side	Total Dose [Gy]	Fractions	Treatment technique
1	77	M	Esophagus cancer	Medial	Center	20	5	TH
2	62	F	Thymus cancer	Medial	Center	54	30	TH
3	52	F	Contralateral axillary involvement in breast cancer recurrence	Lateral	Sinister	50	25	TH
4	60	F	Thymus cancer	Lateral	Sinister	45	25	TH
5	73	M	Small cell lung cancer	Medial	Dexter	45	25	TH
6	85	M	Esophagus cancer	Medial	Sinister	20	5	3DCRT
7	54	M	Esophagus cancer	Medial	Sinister	30	10	3DCRT
8	84	M	Lung cancer	Lateral	Sinister	25	5	3DCRT
9	73	F	Non-small cell lung cancer	Lateral	Dexter	40	8	3DCRT
10	73	F	Small cell lung cancer	Medial	Sinister	45	25	3DCRT

Table 2. Age, gender, diagnose, target location and side, total radiation dose, number of radiotherapy fractions and treatment technique for the abdominal cases.

Case number	Age	Gender	Diagnose	Target location	Target side	Total Dose [Gy]	Fractions	Treatment technique
1	63	M	Malt lymphoma	Lateral	Dexter	24	12	TH
2	71	M	Diffuse large B-Cell lymphoma	Medial	Center	36	12	TH
3	68	F	Liposarcoma	Lateral	Dexter	50	25	TH
4	70	F	Cholangiocarcinoma	Medial	Center	30	10	TH
5	80	M	Cardia ventriculi cancer	Medial	Sinister	20	5	TH
6	37	F	Adrenocortical carcinoma	Lateral	Dexter	50.4	28	3DCRT
7	47	M	Pancreas cancer	Medial	Center	36	12	3DCRT
8	57	F	Liver metastasis	Lateral	Dexter	30	10	3DCRT
9	70	F	Follicular lymphoma	Medial	Dexter	24	12	3DCRT
10	71	F	Corpus cancer	Lateral	Sinister	45	15	3DCRT

4.2. Methods

4.2.1. Tomotherapy treatment planning

All contouring of OAR and PTV were performed by radiation oncologists and treatment planners using Eclipse treatment planning system (Varian). Tomotherapy treatment plans were created in the Tomotherapy planning system version 5.1.1.6. The ROI panel in the Tomotherapy planning station was used for selecting target structures (PTV) and setting overlap priorities for OAR. When two OAR overlapped, the overlapping portion was considered part of the structure with the highest priority. However, when target and OAR overlapped, the overlap volume was considered as a part of both structures. The lasers positions, field width and pitch were chosen in the plan settings panel. For TH plans, a pitch between 0.2-0.5 was used along with a field width of 2.5 cm or 5.0 cm depending on the tumor size. For TD plans a pitch of 0.2 was used and a field width of 5.0 cm for all cases. For TD planning the beam angles panel was used to determining the number of beams and angles to cover the target volume.

The optimizer panel (Figure 4) was used to set the dose objectives and priorities for the target structures and OAR. The prescription dose, penalties and modulation factor limit were also chosen in the optimizer panel. For both TH and TD plans a modulation factor limit of 2 was used.

Several parameters were used in the optimization panel to achieve an optimal plan. One of these parameters was the importance value. The importance value for a ROI affected how important/prioritized a specific ROI was, relative to another ROI. ROIs with importance value of 1 had the lowest importance. Another parameter that affected the optimization process was the penalty. The max dose penalty affected the max dose values, a higher penalty enforced the chosen max dose value. Dose-volume histogram (DVH) penalties and min dose penalties worked in a similar way. To reduce the amount of dose delivered to a specified volume and to achieve a specific dose for a volume, the DVH point pop-up box was used to create DVH points for a ROI. The percentage of the target and OAR that should receive a specific dose was specified and then the point (indicated as circle) was created on the DVH chart (Figure 4). A maximum of three points could be used per ROI.

In the fractionation panel the final dose and the fraction time were obtained for the plan. A normal dose calculation grid (3.90 x 3.90 mm) was used in the optimization process for fast dose calculation. Fine calculation grid (1.95 x 1.95 mm) was used in the final dose calculation to achieve the most accurate resolution for the dose calculation.

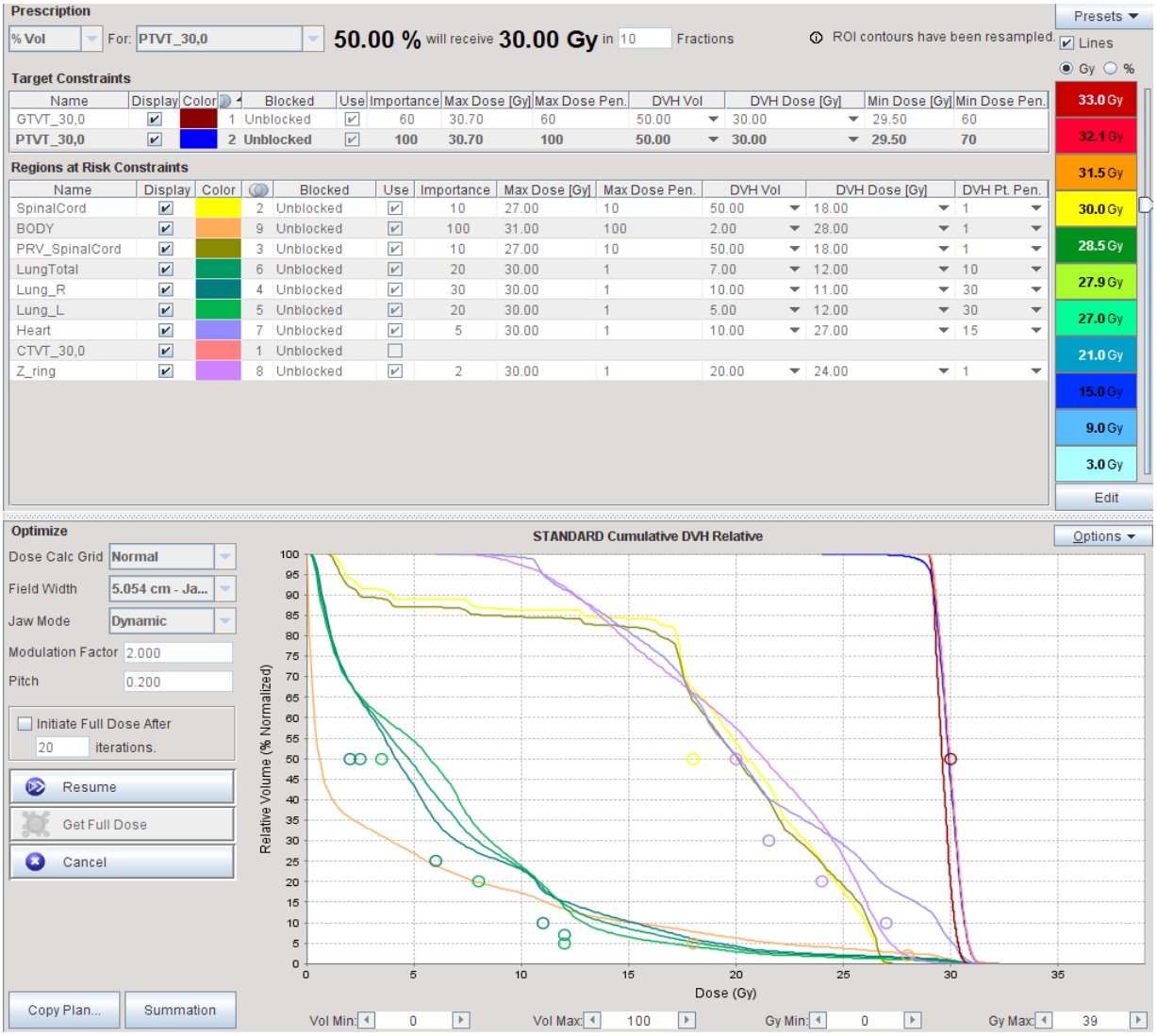

Figure 4. Optimization panel.

4.2.2. Tomodirect: Beam angles

To obtain sufficient target coverage for a TD plan, the number of beams used mainly depended on three factors, the target volume (Appendix B), target location and OAR. In general, large PTV (> 800 cm^3) needed 6-8 beams to obtain sufficient target coverage, compared to small PTV for which 3-4 beams were adequate. In addition, the location of the target and the OAR in its proximity affected the number of beams that was used. For instance, in the thoracic region, when the tumor was centrally located in the body (case 1, Figure 5), three anterior, three posterior and two lateral beams were used (Table 3). For a more ventral located tumor (case 2), three anterior and one posterior beam were used. In contrast, for more lateral and dorsal located tumor (case 8), one anterior beam, two posterior beams and one lateral beam were used. The beam angles were chosen to produce a conformal target coverage and to avoiding unnecessary radiation dose to healthy tissue.

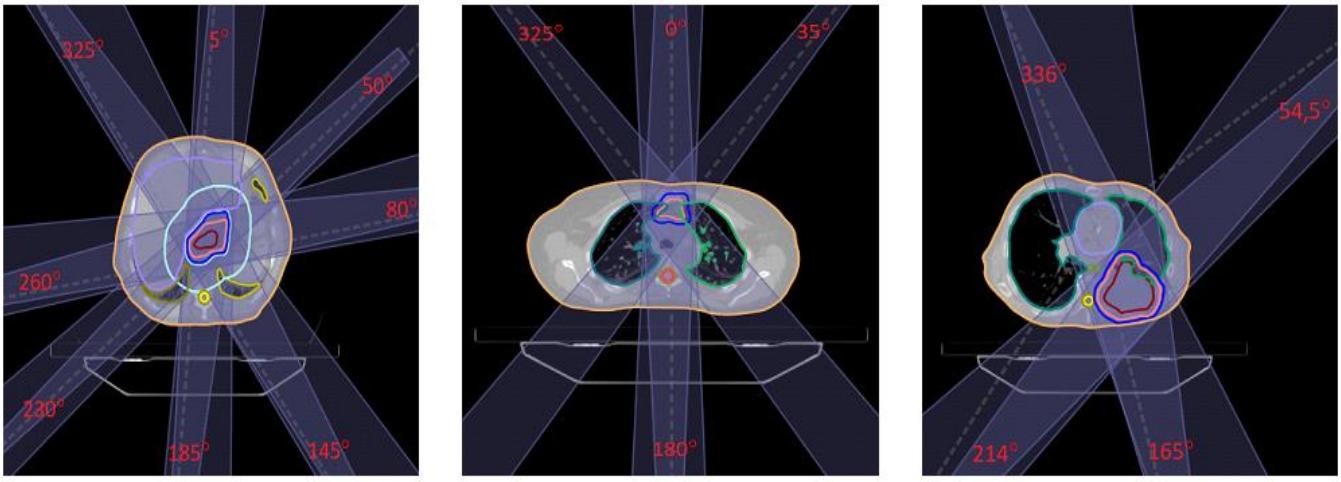

A **B** **C**

Figure 5. Tumor location and beam angles for three thoracic cases. A: Case 1, central located tumor. B: Case 2, ventral located tumor. C: Case 8, lateral and dorsal located tumor.

Table 3. Beam angles for the thoracic cases.

Case number	Beam angle 1 (°)	Beam angle 2 (°)	Beam angle 3 (°)	Beam angle 4 (°)	Beam angle 5 (°)	Beam angle 6 (°)	Beam angle 7 (°)	Beam angle 8 (°)
1	5.0	50.0	80.0	145.0	185.0	230.0	260.0	325.0
2	0.0	35.0	180.0	325.0				
3	28.5	90.0	208.0	333.2				
4	0.0	40.0	80.0	120.0	158.0	205.0	310.0	
5	0.0	60.0	185.0	235.0	327.0			
6	0.0	83.0	123.0	180.0	301.0			
7	29.0	90.0	208.0	333.0				
8	54.5	165.0	214.0	336.0				
9	19.0	193.0	313.2	255.0				
10	0.0	45.0	130.0	180.0	320.0			

For the abdominal cases, when the tumor was located ventral to the body (case 1), two anterior beams and one lateral beam were used (Figure 6, Table 4). For more dorsal located tumor (case 3), two anterior, two posterior and one lateral beam were used. In contrast, for a more central located tumor (case 5), two anterior, one posterior and one lateral beam were used.

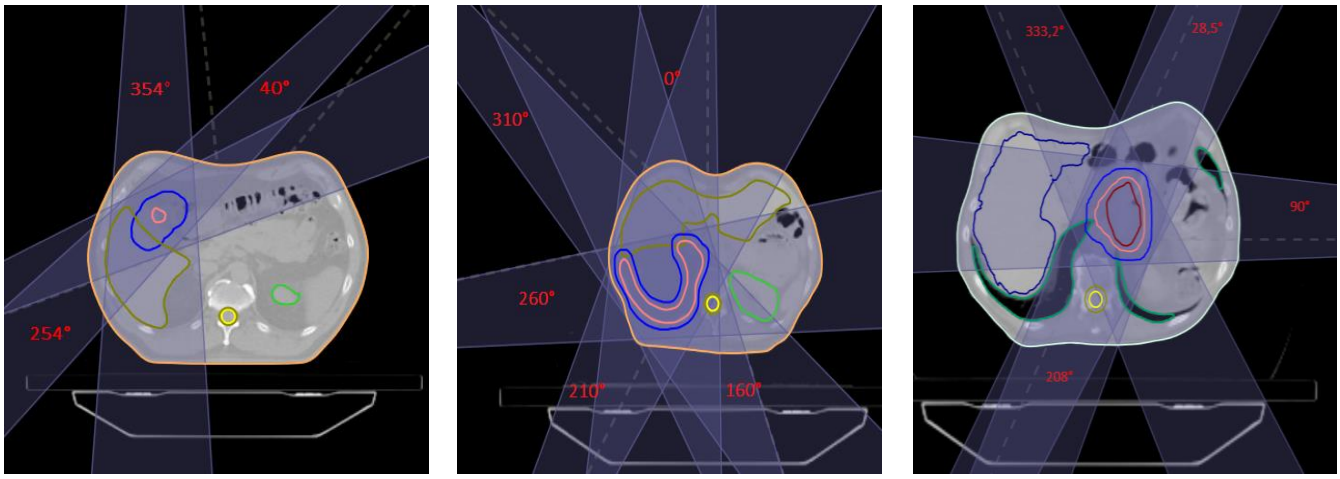

A **B** **C**

Figure 6. Tumor location and beam angles for three abdominal cases. A: Case 1, ventral located tumor. B: Case 3, dorsal located tumor. C: Case 5, central located tumor.

Table 4. Beam angles for the abdominal cases.

Case number	Beam angle 1 (°)	Beam angle 2 (°)	Beam angle 3 (°)	Beam angle 4 (°)	Beam angle 5 (°)	Beam angle 6 (°)
1	40.0	254.0	354.0			
2	0.0	40.0	90.0	180.0	270.0	310.0
3	0.0	160.0	210.0	260.0	310.0	
4	0.0	74.0	180.0	315.0		
5	28.5	90.0	208.0	333.2		
6	27.0	175.0	225.0	334.0		
7	0.0	84.0	180.0	315.0		
8	160.0	250.0	340.0			
9	0.0	34.0	180.0	322.0		
10	0.0	120.0	330.0			

4.2.3. 3DCRT: Beam angles

The 3DCRT treatment plans were created by treatment planners in the radiation therapy building at Skåne university hospital. The chosen beam angles were based on the treatment planners' own experience to obtain a clinical accepted treatment plan. For the thoracic cases (case 6-10, Table 1) 3-5 beams were adequate for a clinical accepted plan (Table 5). For the abdominal cases (case 6-10, Table 2), the treatment planners used 2-5 beams (Table 6).

Table 5. Beam angles for the thoracic cases for the 3DCRT plans.

Case number	Beam angle 1 (°)	Beam angle 2 (°)	Beam angle 3 (°)	Beam angle 4 (°)	Beam angle 5 (°)
6	0	60	90	120	180
7	40	100	180		
8	20	75	130	180	
9	12	200	260	305	
10	0	45	135	180	

Table 6. Beam angles for the abdominal cases for the 3DCRT plans.

Case number	Beam angle 1 (°)	Beam angle 2 (°)	Beam angle 3 (°)	Beam angle 4 (°)	Beam angle 5 (°)
6	33	72	134	210	322
7	0	87	173	273	
8	14	173	229	325	
9	0	75	172		
10	120	330			

4.2.4. Dose constraints and objectives

A main goal of the treatment planning is to achieve sufficient target coverage. In our study, this is represented by the objective that 98% of PTV volume should receive at least 95% of the prescribed dose ($V_{95\%} \geq 98\%$). The maximum dose delivered should not exceed 110%. The dose constraints used for OAR (Table 7) is obtained from QUANTEC (23).

Table 7. Dose constraints for OAR from QUANTEC.

Organs	Volume segmented	Dose [Gy]
Spinal cord	Partial organ	$D_{max} < 50$
Lung	Whole organ	Dmean ≤ 20
Esophagus	Whole organ	Dmean < 34
Heart	Whole organ	Dmean < 26
Liver	Whole liver	Dmean < 30-32
Kidney	Bilateral whole kidney	Dmean < 15-18

4.2.5. Plan comparison and statistical analysis

TD plans were compared with TH and 3DCRT plans regarding the PTV coverage ($V_{95\%}$), HI, CI, mean absorbed dose to OAR and beam-on time.

For the thoracic cases, the mean absorbed dose to the heart and to the right and left lung were evaluated separately. For the abdominal cases, the mean absorbed dose to the right and left kidney and liver were evaluated separately. To test the statistical significance of our results, one-sided sign test was performed. The significance level chosen was 5% ($\alpha < 0.05$). H_0: TD

and the other used treatment technique (TH or 3DCRT) are equal. H_1: TD is superior to the other used treatment technique.

4.2.6. Delta^4 measurements

4.2.6.1. Preparation before measurements

Before the Delta^4 phantom+ measurements, DQA plans were generated in the DQA software version 5.1.1.5. A DQA plan was created for each plan, for which the dose distribution was calculated on the phantom image volume.

4.2.6.2. Plan measurements

The Delta^4 phantom+ was positioned on the tomotherapy treatment couch using the red lasers (transversal, sagittal and coronal) according to the position of the phantom volume defined in the DQA setup. A MVCT was acquired for setup verification of the phantom position and registered with the kVCT. The next step was to measure the plans and use gamma analysis (global gamma) for evaluating the difference between delivered and measured dose distribution using Scandidos Delta^4 software (version October 2016). Our clinical acceptance criteria for gamma evaluation is 3% dose difference and 2 mm distance-to agreement, with 90% approved data points at a threshold level of 15%-500%. All points with a dose less or above the threshold were discriminated.

4.2.7. Angular dependence of the Delta^4

In order to check the Delta^4 phantom+ response to different beam angles, ten QC plans were created on a cylindrical phantom with two opposite beams each, with a 10º rotational shift for each consecutive plan. In the first case, the target was centrally located (Figure 7A) to verify the angle dependence of the Delta^4 phantom+. Afterwards, the target was laterally located (Figure 7B) to investigate the angle dependence and target position dependence of the Delta^4 phantom+. The QC plans were created and measured in a similar way as the treatment plans in the tomotherapy machine.

A B

Figure 7. Target location in the phantom. A: Central target. B: Lateral target.

4.2.8. Robustness

To get an insight of the robustness of TD compared to TH for the planned cases, Hexamotion (Figure 8) was used. Hexamotion is a device used to simulate breathing motion. In this case, it was used to set the Delta^4 phantom+ in motion. A sinusoidal waveform with the amplitude of +5 mm and a repetition rate of three seconds in cranio-caudal direction was used in the first

measurement of the TD and TH plan. Secondly, a sinusoidal waveform with an amplitude of +20 mm was used along with a repetition rate of seven seconds in cranio-caudal direction. And finally, a sinusoidal waveform with an amplitude of ±5 mm was used with a repetition rate of two seconds in both cranio-caudal and anterior-posterior direction. All the measurements were only performed for a single thoracic plan (case 4) with the field width 5.0 cm.

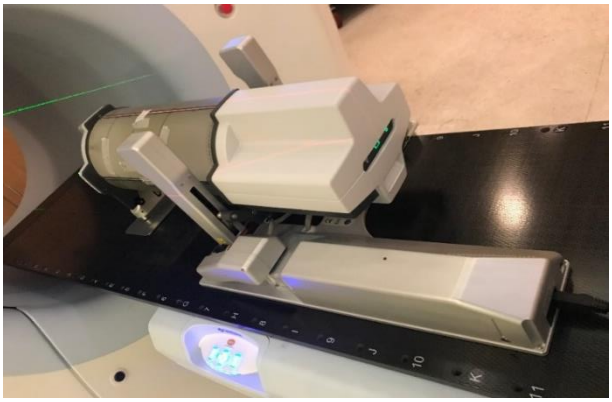

Figure 8. Hexamotion in conjunction with the Delta^4 phantom+.

5. Results

5.1. Plan comparison

5.1.1. Thorax

5.1.1.1. TH vs TD

The one-sided sign test showed no significance at $p<0.05$ for comparison of PTV coverage ($p=0.3$) and HI ($p=0.5$) between TH and TD plans (Table 8). The p-value for comparison of CI between TH and TD was 0.02, which means that TH had significant better conformity than TD.

Table 8. Comparison of PTV coverage ($V_{95\%}$), HI and CI for the thoracic cases between TH and TD plans.

		Case 1	**Case 2**	**Case 3**	**Case 4**	**Case 5**
PTV coverage $V_{95\%}$ (%)	TH	99.0	97.2	97.8	97.1	99.3
	TD	**99.0**	**99.1**	**97.8**	**99.7**	**97.6**
HI	TH	0.1	0.1	0.1	0.1	0.1
	TD	**0.1**	**0.1**	**0.1**	**0.1**	**0.1**
CI	TH	0.9	0.8	0.7	0.8	1.0
	TD	**0.8**	**0.6**	**0.7**	**0.7**	**0.9**

The PTV coverage ($V_{95\%}$) for the planned cases is shown in Figure 9, each marker corresponds to one paired plan/case. Three TH and two TD cases were below the clinical threshold (the dashed line in the figure). In terms of mean absorbed doses to OAR (Figure 10), the one-sided sign test showed no statistical significance for the comparison between TD and TH (right lung $p=0.2$, left lung $p=0.7$, Heart $p=0.7$). The mean absorbed dose to the right lung (case 5) were above the dose constraints ($D_{mean}< 20$ Gy) obtained from QUANTEC due to the lateral target location. Similarly, for case 4, the left lung obtained an absorbed dose above the QUANTEC constraints due to the lateral target location.

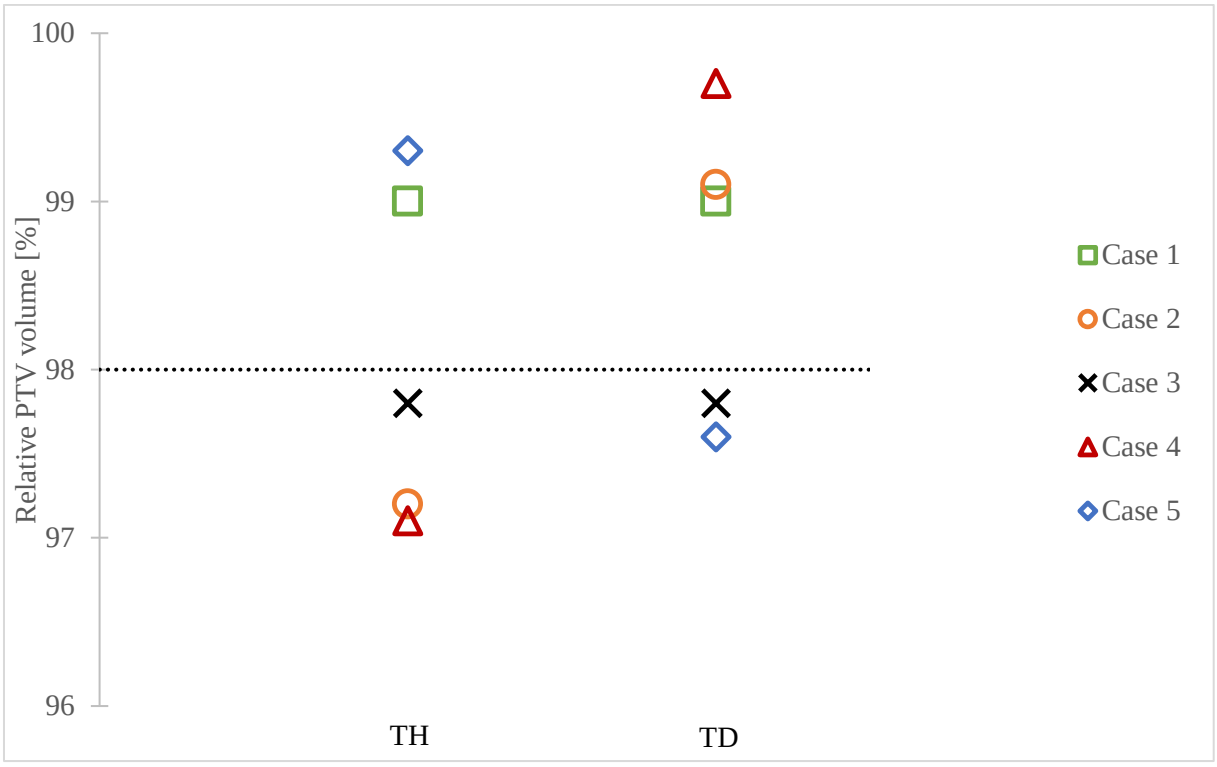

Figure 9. PTV coverage ($V_{95\%}$) for thoracic cases for TH and TD plans. The dashed line is the clinical threshold for acceptable PTV coverage. Each marker corresponds to one paired plan.

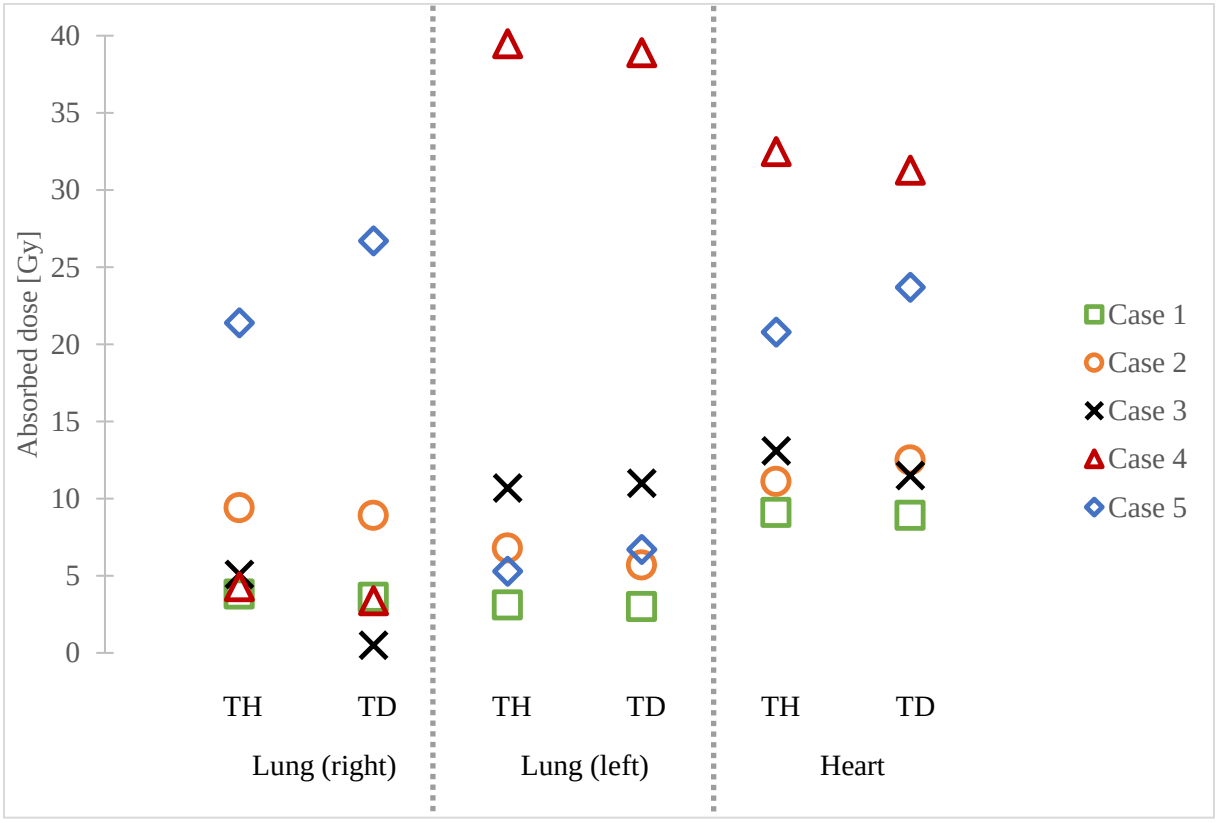

Figure 10. Comparison of mean absorbed dose to right lung, left lung and heart between TH and TD plans. Each marker corresponds to one paired plan.

The results (Figure 11) showed that for case 2, 3 and 5, the beam-on time was shorter for TD than TH. In case 1, the beam-on time for the TD plan was one minute longer than TH, and in case 4, the beam-on time was approximately equal in both TD and TH plan. Though there seemed to be a general gain in treatment time with TD compared to TH, the used statistical test showed no significant difference (p=0.7).

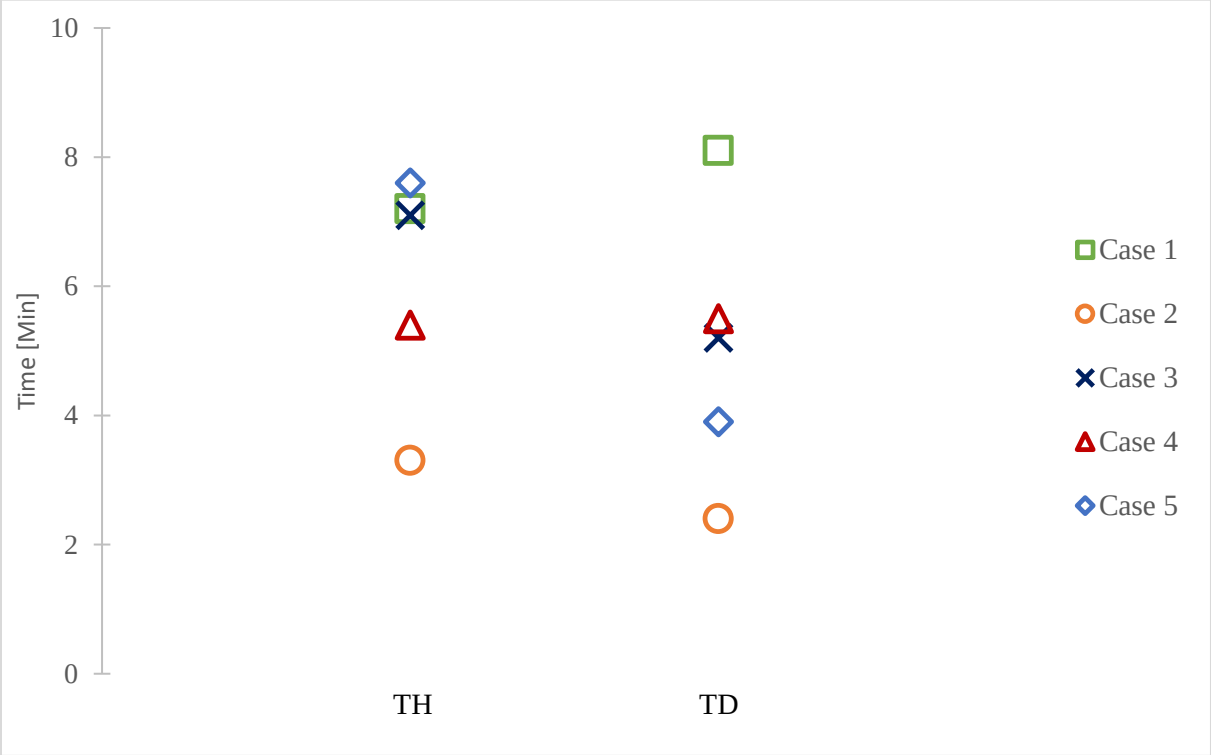

Figure 11. Comparison of beam-on times between TH and TD plans. Each marker corresponds to one paired plan.

5.1.1.2. 3DCRT VS TD

The PTV coverage was significantly better (p=0.01) for TD plans relative to 3DCRT (Table 9). The HI (p=0.2) and CI (p=0.2) were equivalent for TD and 3DCRT plans.

Table 9. Comparison of PTV coverage ($V_{95\%}$), HI and CI for the thoracic cases between 3DCRT and TD plans.

		Case 6	Case 7	Case 8	Case 9	Case 10
PTV coverage $V_{95\%}$ (%)	3DCRT	98.9	95.5	97.0	91.8	96.0
	TD	**99.3**	**99.9**	**99.9**	**97.3**	**99.3**
HI	3DCRT	0.1	0.1	0.1	0.3	0.1
	TD	**0.1**	**0.1**	**0.1**	**0.1**	**0.1**
CI	3DCRT	0.6	0.8	0.7	0.9	0.6
	TD	**0.8**	**0.8**	**0.9**	**0.8**	**0.7**

For all 3DCRT plans, except case 6, the PTV coverage was below the clinical threshold (Figure 12). The mean absorbed dose (Figure 13) to the right lung (contralateral in 4 of 5 cases) were equal for 3DCRT and TD (p=0.7). A significant decrease in mean absorbed dose to left lung (ipsilateral in case 6,7,8 and 10) was obtained in TD plans relative to 3DCRT plans (p=0.01). No information about heart mean absorbed doses was obtained for case 9 and 10, and the sign test could not be performed due to the small sample size (less than 5). There was a significant increase (p=0.01) in beam-on time (Figure 14) for TD plans (3.0-9.6 min) compared to 3DCRT plans (2.3-4.1 min).

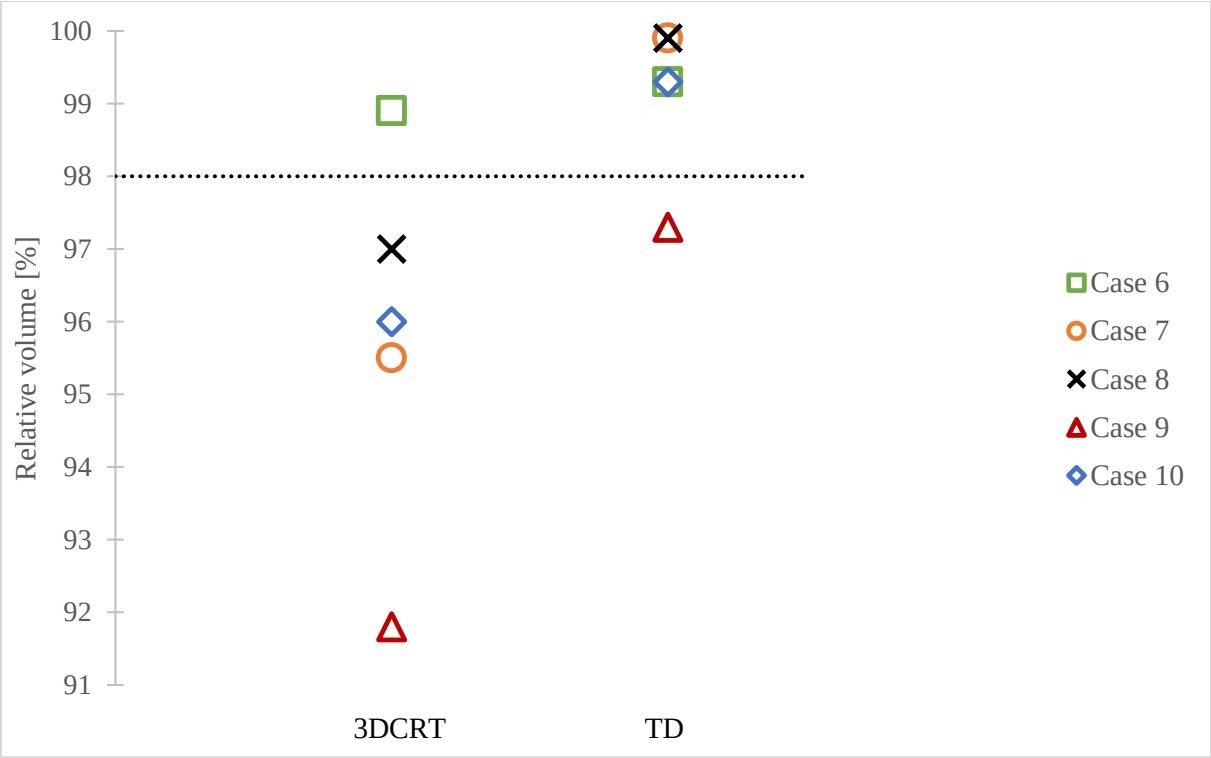

Figure 12. PTV coverage ($V_{95\%}$) for thoracic cases for 3DCRT and TD plans. The dashed line is the clinical threshold for acceptable PTV coverage. Each marker corresponds to one paired plan.

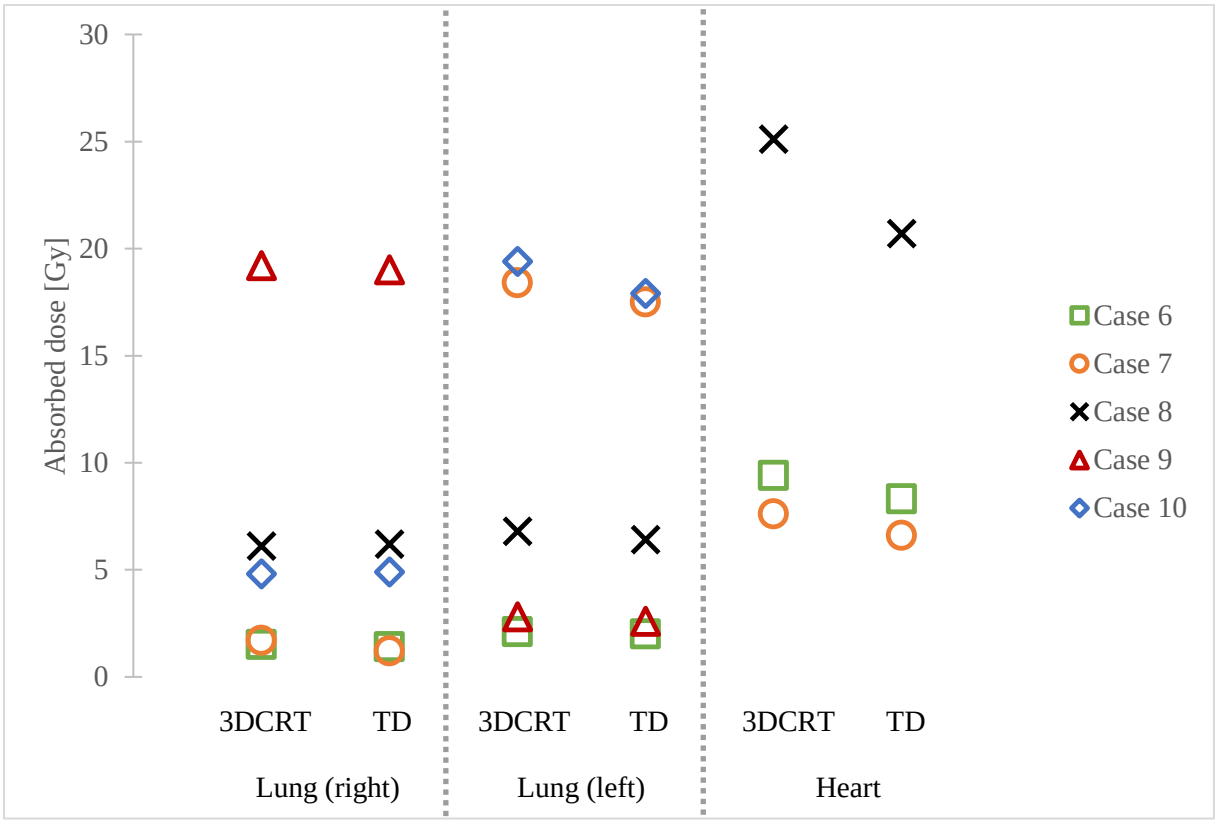

Figure 13. Comparison of mean absorbed dose to right lung, left lung and heart between 3DCRT and TD plans. Each marker corresponds to one paired plan.

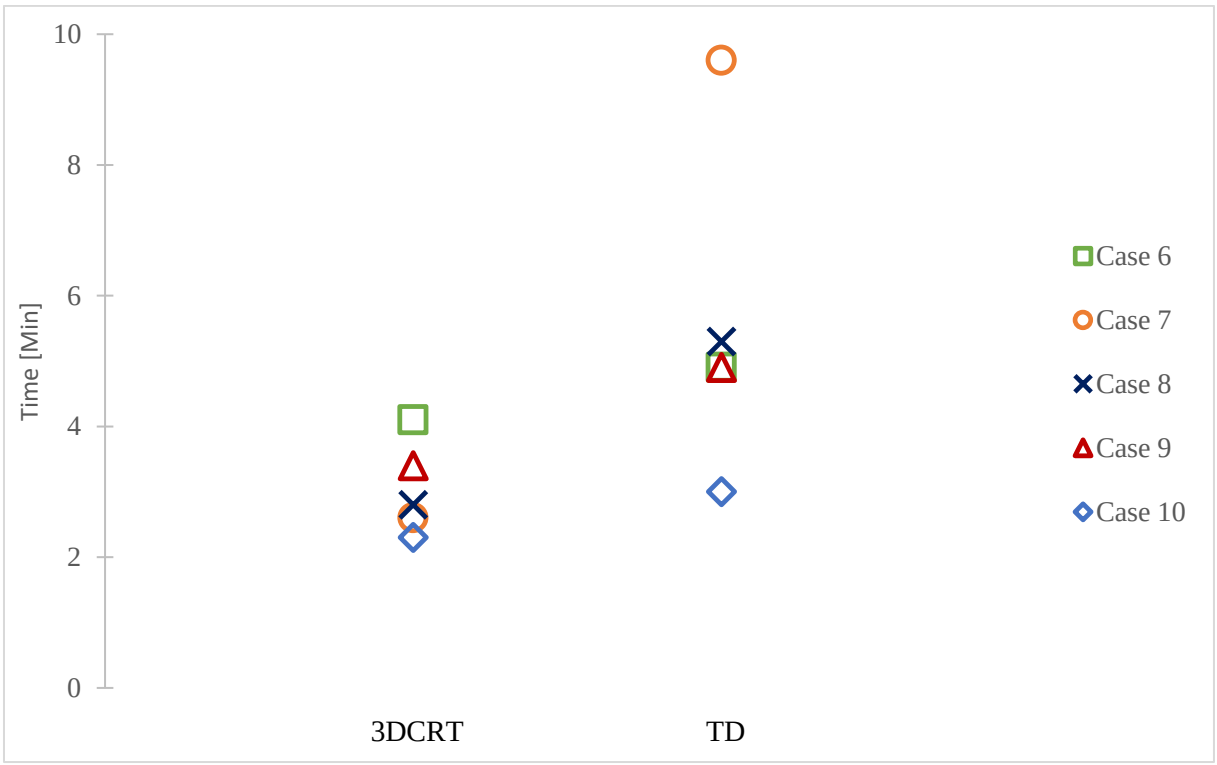

Figure 14. Comparison of beam-on times between 3DCRT and TD plans. Each marker corresponds to one paired plan.

5.1.2. Abdomen

5.1.2.1. TH VS TD

Our results showed (Table 10) that TH had better HI than TD (p=0.04). The PTV coverage was better for TH compared to TD (p=0.01). However, both TH and TD had clinical acceptable PTV coverage (Figure 15). Both tomotherapy modalities showed equivalent conformity in the abdominal region.

Table 10. Comparison of PTV coverage ($V_{95\%}$), HI and CI for the abdominal cases between TH and TD plans.

		Case 1	Case 2	Case 3	Case 4	Case 5
PTV coverage $V_{95\%}$ (%)	TH	100.0	99.4	99.9	100.0	99.1
	TD	**99.8**	**98.6**	**98.8**	**99.1**	**98.9**
HI	TH	0.0	0.1	0.0	0.0	0.1
	TD	**0.1**	**0.1**	**0.1**	**0.1**	**0.1**
CI	TH	0.9	0.8	0.7	0.8	0.8
	TD	**0.8**	**0.8**	**0.6**	**0.7**	**0.9**

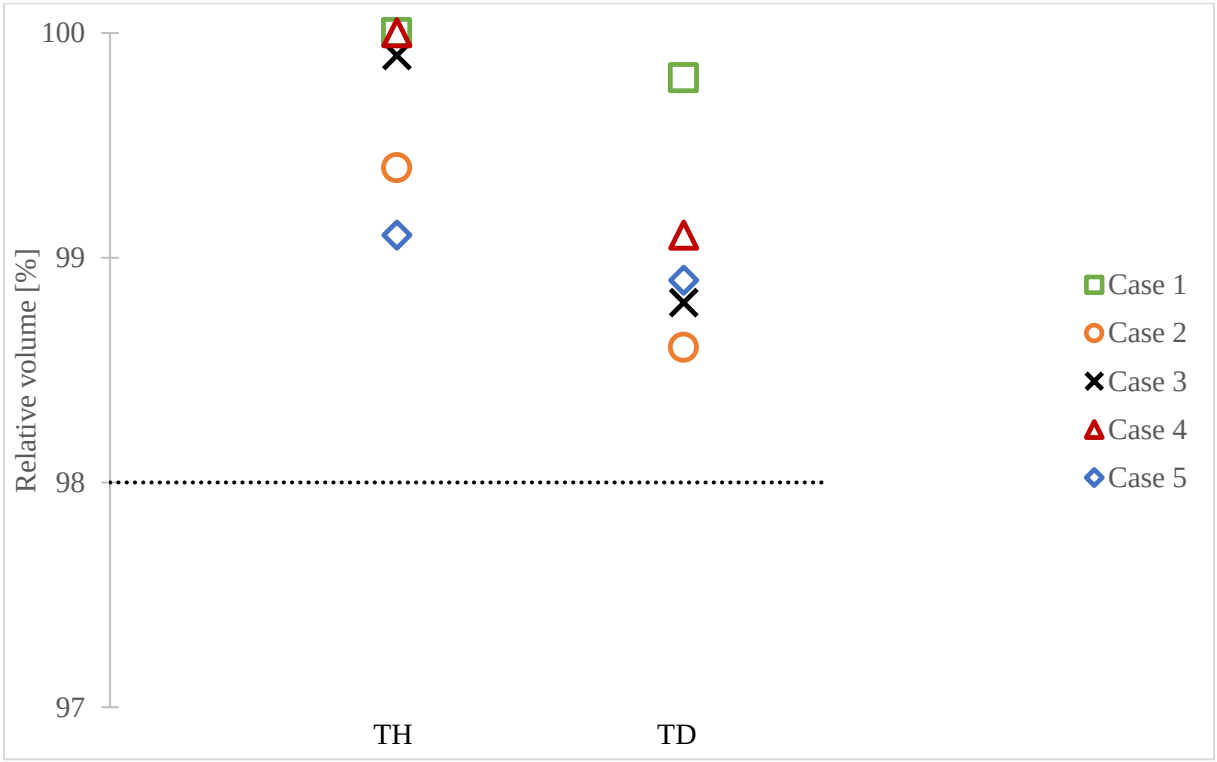

Figure 15. PTV coverage ($V_{95\%}$) for abdominal cases for TH and TD plans. The dashed line is the clinical threshold for acceptable PTV coverage. Each marker corresponds to one paired plan.

There were no statistical differences of the mean absorbed dose to the left kidney (p=0.7) and the liver (p=1.0) between TH and TD plans (Figure 16). Due to too few data points, the sign test could not be performed for the right kidney. The beam-on times (Figure 17) were significantly shorter (p=0.03) for TD (2.4-5.4 min) compared to TH (4.1-8.6 min).

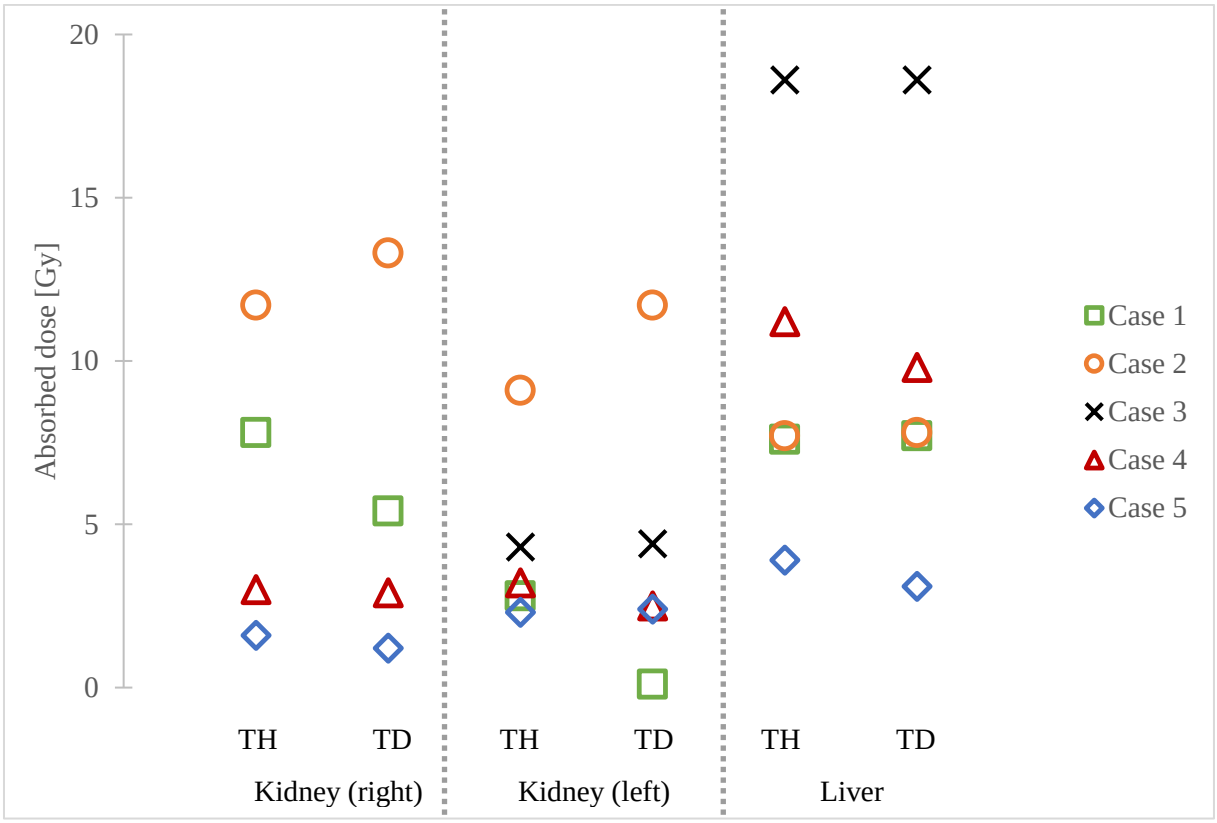

Figure 16. Comparison of mean absorbed dose to right kidney, left kidney and liver between TH and TD plans. Each marker corresponds to one paired plan.

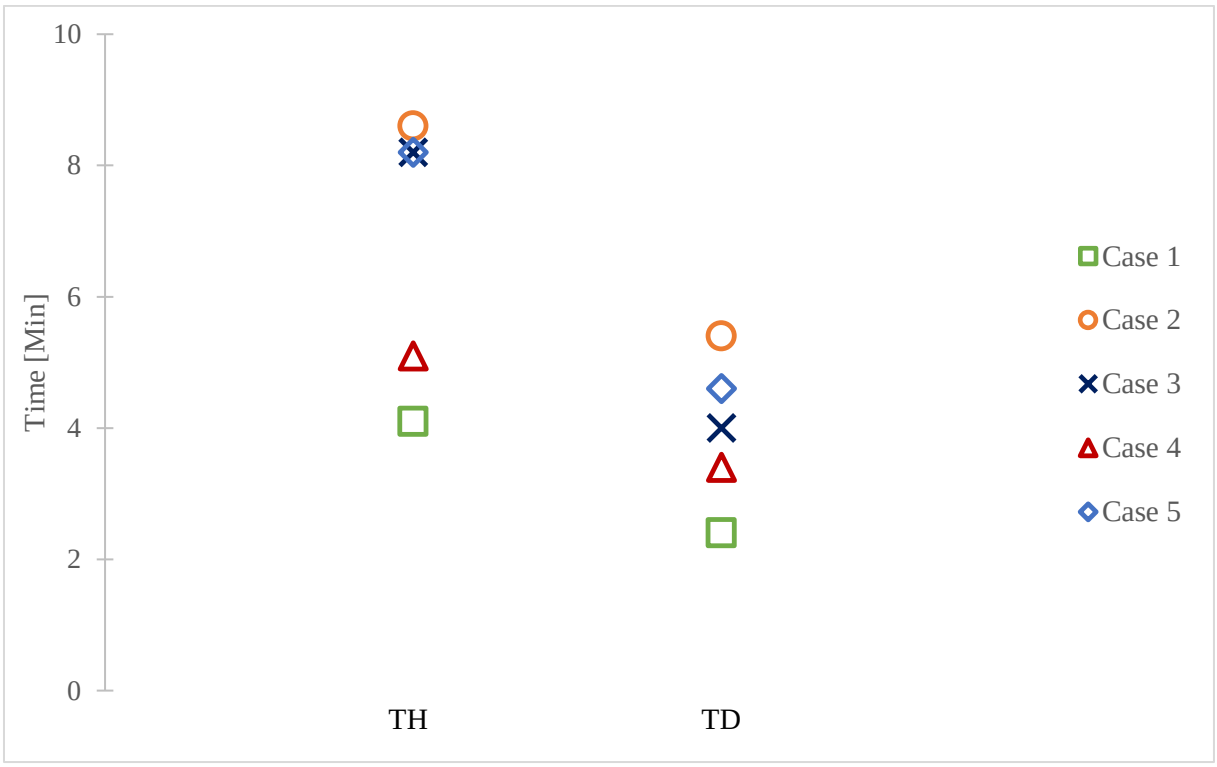

Figure 17. Comparison of beam-on times between TH and TD plans. Each marker corresponds to one paired plan.

5.1.2.2. 3DCRT vs TD

Our results showed (Table 11) that the PTV coverage was significantly higher for TD plans than 3DCRT (p=0.01). We can notice (Figure 18) that all 3DCRT plans had a PTV coverage that was below the clinical acceptable threshold. In terms of HI and CI, there was no statistical difference between TD and 3DCRT (HI: p=0.08, CI: p=0.3).

Table 11. Comparison of PTV coverage, HI and CI for the abdominal cases between 3DCRT and TD plans.

		Case 6	Case 7	Case 8	Case 9	Case 10
PTV coverage $V_{95\%}$ (%)	3DCRT	91.3	96.1	75.6	96.7	96.8
	TD	**98.8**	**99.5**	**99.5**	**99.8**	**99.9**
HI	3DCRT	0.1	0.1	0.4	0.1	0.1
	TD	**0.1**	**0.1**	**0.1**	**0.1**	**0.0**
CI	3DCRT	0.7	0.7	1.2	0.3	0.7
	TD	**0.7**	**0.8**	**0.7**	**0.6**	**0.7**

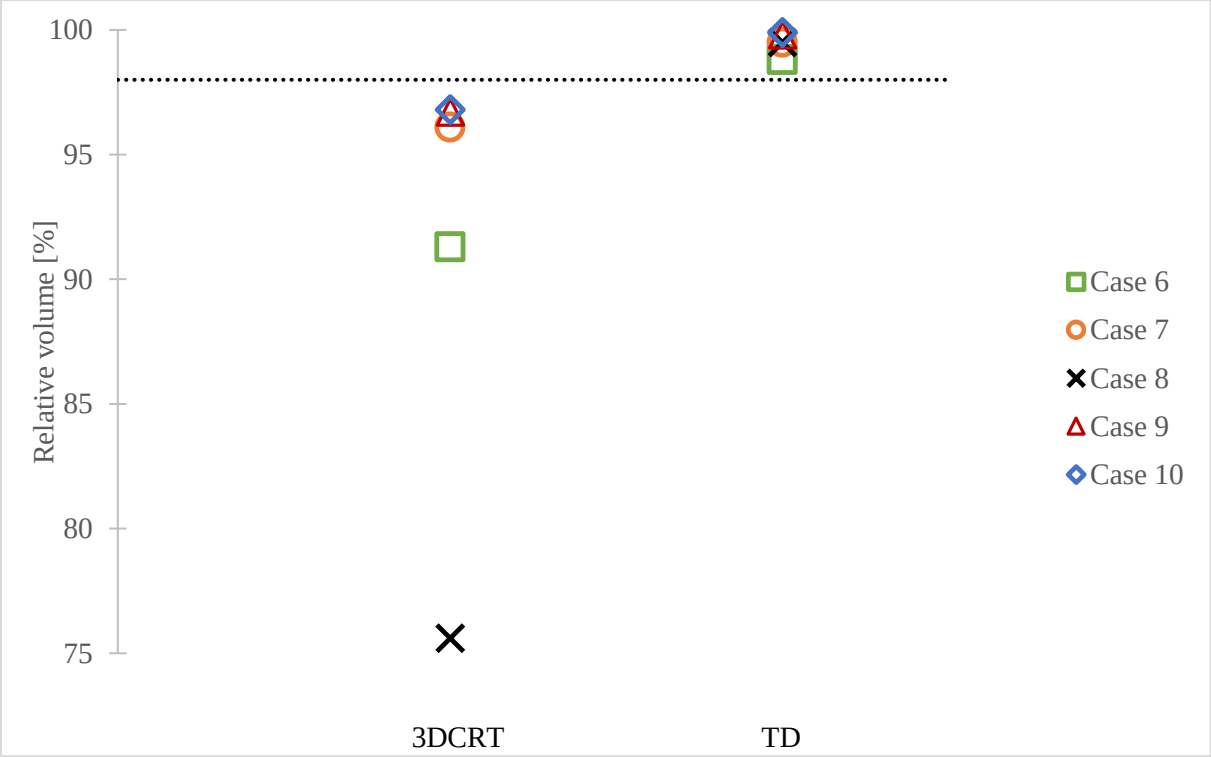

Figure 18. PTV coverage for abdominal cases for 3DCRT and TD plans. The dashed line is the clinical threshold for acceptable PTV coverage. Each marker corresponds to one paired plan.

The mean absorbed dose (Figure 19) for left kidney and liver were equivalent for TD and 3DCRT plans (left kidney: p=0.09, liver: p=0.5). Due to too few data points, the sign test could not be performed for the right kidney. There was no statistical difference in beam-on time (p=0.2) between TD and 3DCRT (Figure 20).

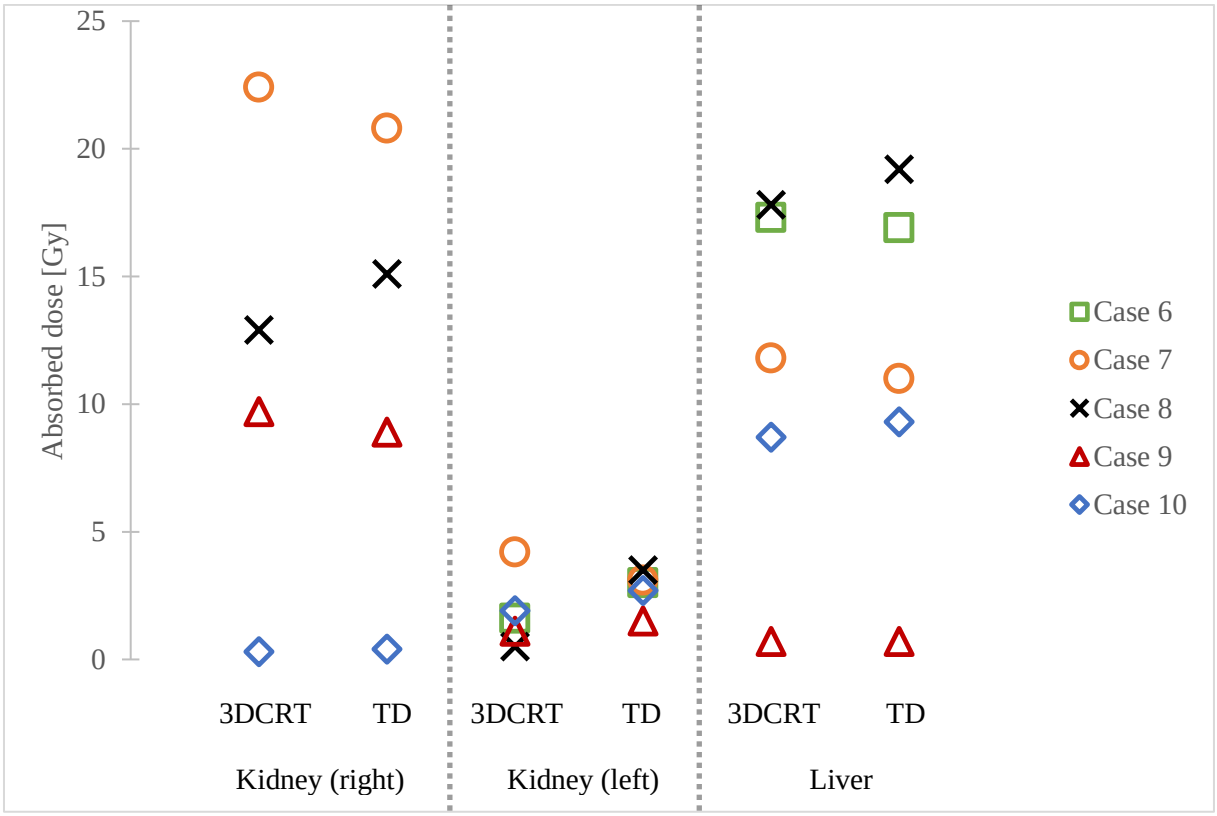

Figure 19. Comparison of mean absorbed dose to right kidney, left kidney and liver between 3DCRT and TD plans. Each marker corresponds to one paired plan.

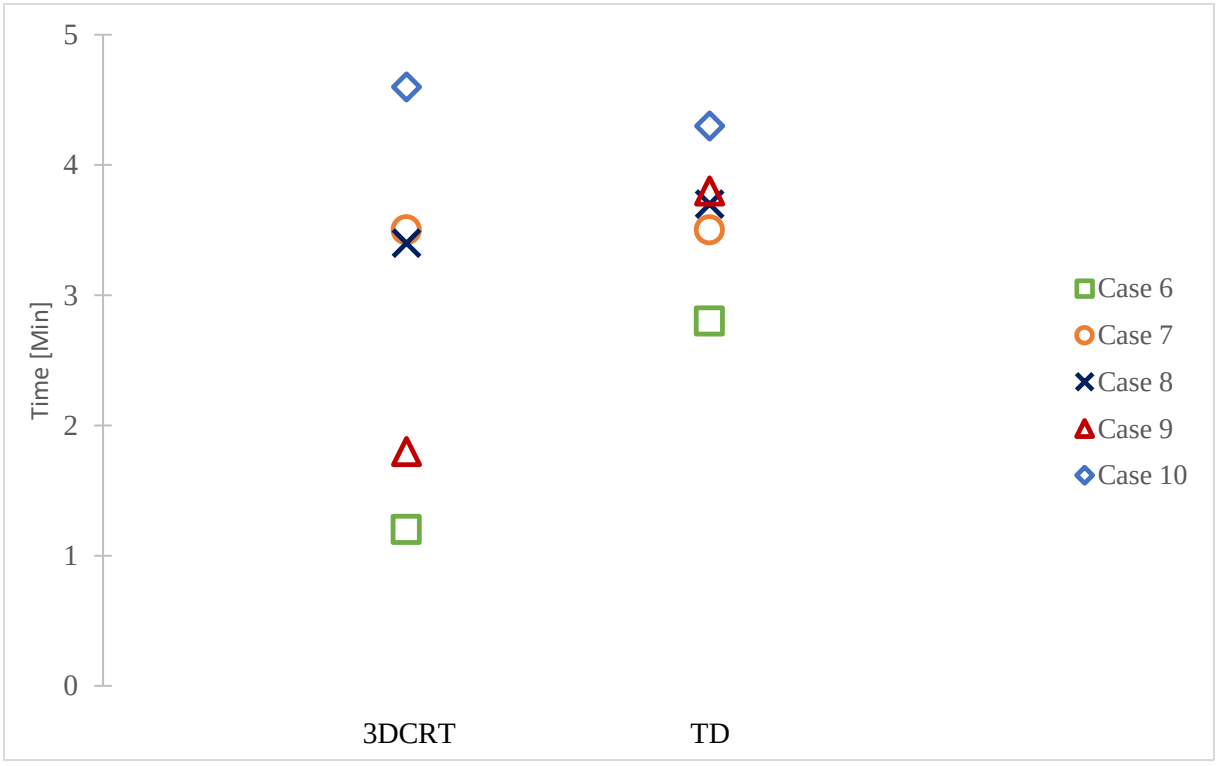

Figure 20. Comparison of beam-on times between 3DCRT and TD plans. Each marker corresponds to one paired plan.

5.2. QC

5.2.1. Treatment plan measurements

Our results show (Figures 21 and 22) that the gamma pass rates were equivalent for TH and TD, in both thoracic and abdominal region, except for case 2 in the thoracic region. For case 2, a gamma pass rate of 96.9% was obtained for the TD plan relative to 100.0% for the TH plan. However, the result was well above the clinical acceptable threshold.

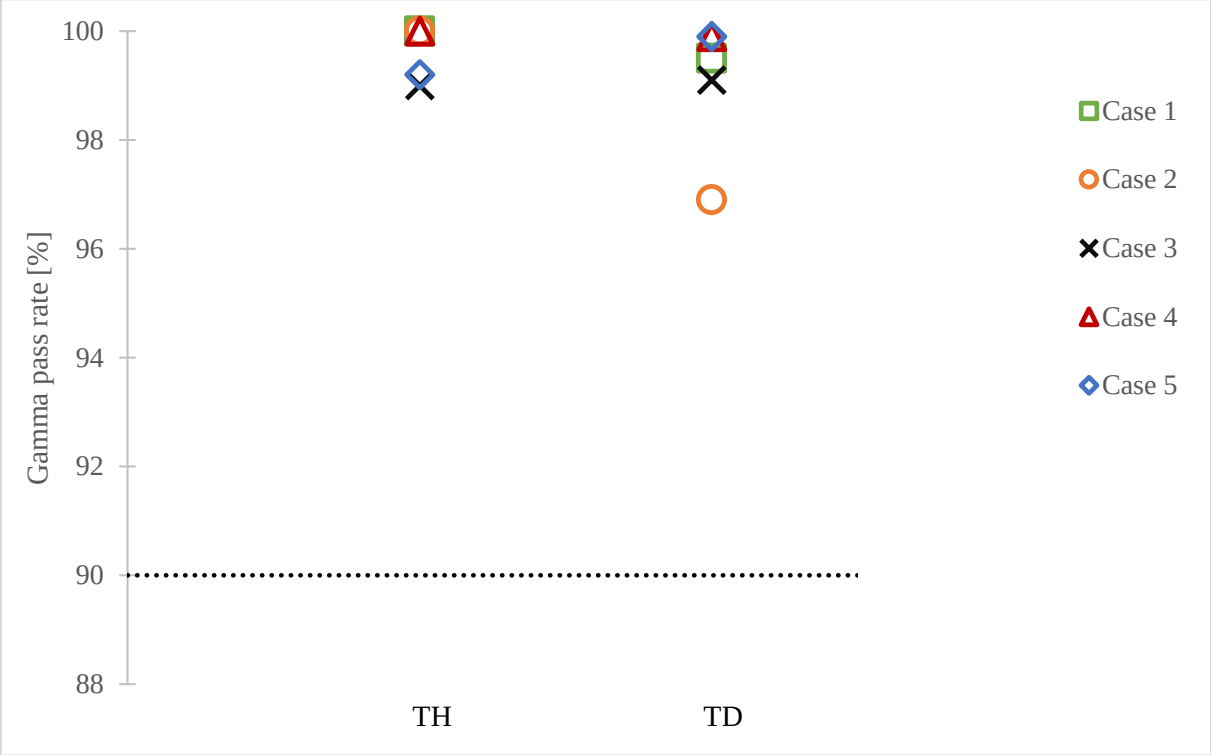

Figure 21. Gamma pass rate for Delta^4 phantom+ QC measurements of TH and TD plans in the thoracic region. The dashed line is the clinical acceptable threshold. Each marker corresponds to one paired plan.

Figure 22. Gamma pass rate for Delta[4] phantom+ QC measurements of TH and TD plans in the abdominal region. The dashed line is the clinical acceptable threshold. Each marker corresponds to one paired plan.

5.2.2. Angular dependence of the Delta[4]

Table 12 and Figure 23 show the gamma pass rates from the measurements of the QC plans with two opposite beams each for central and lateral located target. For the central located target, only plan 1-4 were above the clinical acceptable threshold. For the lateral target, only plan 1-3 were above the clinical acceptable threshold.

Table 12. Gamma pass rate for ten QC plans with two opposing beams at different angles for central and lateral located target.

Plan nr	Angles [°]	Central target $\gamma_{3\%,2mm}$[%]	Lateral target $\gamma_{3\%,2mm}$[%]
1	90–270	96.1	91.1
2	100–280	100.0	99.5
3	110–290	99.8	98.4
4	120–300	97.8	84.1
5	130–310	86.6	65.5
6	140–320	71.0	72.2
7	150–330	79.5	76.8
8	160–340	70.8	67.6
9	170–350	68.0	73.4
10	180–360	69.7	68.8

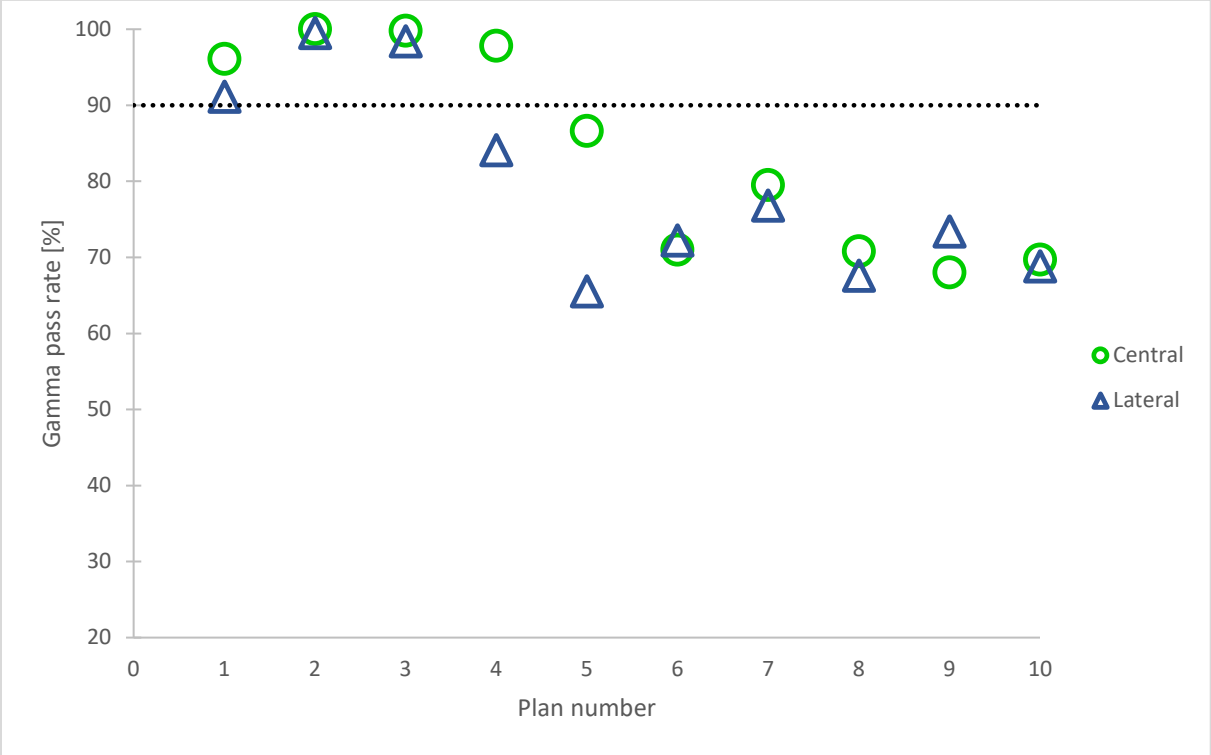

Figure 23. Gamma pass rate for the QC plans with two opposing beams at different angles. The dashed line is the clinical acceptable threshold. The QC plans with central target are indicated by the green circles. The QC plans with lateral target are indicated by the blue triangles.

5.3. Robustness

The gamma pass rates for TH and TD plan measurement for cranio-caudal motion of a sinusoidal waveform with an amplitude of 0 mm (no motion), +5 mm and +20 mm (Table 13), were equivalent. The analysis of the dose profiles and the diode arrays showed that the gamma fails in the high dose region for both plans. For the waveform with the amplitude of +20 mm, the gamma pass rate for both the TH and TD plan was below the clinical acceptance threshold of a 90% approved data points. The gamma pass rate decreased more for the TD plan (83.5%) than for the TH plan (96.1%), when the phantom was set in cranio-caudal and anterior-posterior motion (Table 14).

Table 13. Comparison of gamma pass rates between TH and TD for motion in cranio-caudal for a sinusoidal waveform with an amplitude of 0 mm, +5 mm and +20 mm.

Amplitude [mm]	$\gamma_{3\%,2mm}$ [%]	
	TH	**TD**
0	99.7	99.4
+5	96.3	96.5
+20	66.2	64.4

Table 14.Comparion of gamma pass rates between TH and TD for motion in cranio-caudal and anterior-posterior caudal for a sinusoidal waveform with an amplitude of 0 mm and ±5 mm.

Amplitude [mm]	$\gamma_{3\%,2mm}$ [%]	
	TH	**TD**
0	99.7	99.4
±5	96.1	83.5

6. Discussion

Many studies have investigated the use of TD for breast cancer irradiation (11) (24), but only few studies have investigated the use of TD in the thoracic and abdominal region. In this study an investigation of the use of TD for several diagnoses in the thoracic and abdominal region was performed.

6.1. Plan comparison

The treatment plan comparison showed that both TH and TD could achieve an excellent PTV coverage in the abdominal region. In contrast, in the thoracic region the PTV coverage for both TH and TD plans were below the clinical threshold for some cases. Despite the use of only few beam angles in TD plans, the mean absorbed dose to OAR were almost equal for both techniques. To achieve acceptable PTV coverage in central located target with a lot of OAR in proximity, the TD fields had to intersect the OAR before reaching the target, resulting in dose being delivered also to the OAR. The TH technique provides greater flexibility for intensity modulation of the dose delivery using beams from all directions. As mentioned earlier in the theory section, the drawback of TH is the large dose bath. This was also shown in a study by Murai et al (2013), where TH was shown to deliver low-dose radiation to larger lung volume than TD (25).

Whereas the PTV coverage and the mean absorbed dose to OAR were comparable between TH and TD, the TH plans showed better conformity in the thoracic region and better homogeneity in the abdominal region. This is due to the greater number of beam angles available in the TH plan. The number of beam angles in the TD plans affected the beam-on time, the more beams the longer beam-on time. To obtain sufficient target coverage for large tumors more beams were needed than for small tumors. In the thoracic region, the PTV volume range was 362.8-2449.6 cm^3 and 4-8 beams were used, which resulted in almost equivalent beam-on time for TD and TH plans. In the abdominal region, the PTV range was 441.4-1511.3 cm^3 and 3-6 beams were used, which resulted in shorter beam-on time for TD than TH plans.

The paired plan comparison between TD and 3DCRT plans showed that TD plans had superior PTV coverage compared to 3DCRT plans. This result was in agreement with results from previous studies (26) (13). The homogeneity and conformity were almost equivalent for TD and 3DCRT plans. Interestingly for case 8, CI was equal to 1.2 for the 3DCRT plan (Table 11), which is likely due to the low PTV coverage of 75.6%.

Generally, TD did not improve the mean absorbed dose to OAR compared to 3DCRT. Although, in the thoracic region, the result showed that the left lung obtained a lower mean absorbed dose in TD plans relative to 3DCRT plans. The beam-on times for TD plans in the thoracic region was significantly higher than 3DCRT plans which was due to as mentioned before the number of beams used. The beam-on times for the plans in the abdominal region were comparable. There were some common beam angles that were used both in TD planning and 3DCRT planning (Table 3-6), but overall the beam angles were different. An explanation for this is that the 3DCRT plans and TD plans were performed by different planners.

Overall, like any irradiation technique, TD has its advantages and disadvantages. A trade-off between these should be assessed before the choice of technique.

6.1.1. The impact of the treatment planner

The treatment planners that performed the 3DCRT plans and TH plans have been working with clinical treatment planning for a long time. For example, in 3DCRT, the treatment planners have experience of which beam angles that should be used for different target locations, target volumes and OAR in proximity to obtain clinical accepted treatment plans. However, the treatment planners are often limited by the time to perform optimal treatment plans. The treatment plans are clinical accepted, which is good enough but not always optimal. The TD plans were performed by an unexperienced student (with supervision of an experienced physicist), the student had the time to experiment with different beam angles and parameters (i.e. importance value) to investigate which treatment plan is better. The fact that the treatment planners and the student do not had the same conditions may had influenced the results. For further work, it will be interesting to investigate the personal impact to the results if the same planner performs both 3DCRT, TH and TD plans.

6.2. QC

The results from the QC of the clinical treatment plans showed equivalent (and clinical acceptable) gamma pass rates for TH and TD plans. Perhaps, more interesting were the results for the measurements of the TD QC plans with only two opposing beams, with the target in central respective lateral position (Table 12 and Figure 23). The results for the central located target showed that the response of the Delta^4 phantom+ was angular dependent. For the plan with angles 100°-280°, the Delta^4 phantom+ response was excellent. Surprisingly, the response of the Delta^4 phantom+ for the angles 90°-270° was also good ($\gamma_{3\%,2mm}$: 96,1%). This result was unexpected because the detectors are arranged in two orthogonal planes (horizontal and vertical), and it was expected that the detectors in the plane parallel to the incident beams block each other. The response was worst for the plans with the angles 170°-350° and 180°-360° (same as 0°). A possible explanation for this, was (as mentioned before) that several detectors were blocking each other in the plane parallel to the incident beams. The diodes' inherent angular sensitivity to radiation was corrected for by the Delta^4 software, but the result showed that the correction does not work as desired for the TD QC plans. This also explains the QC result for the clinical treatment plan, case 2 (Figure 21, $\gamma_{3\%,2mm}$: 96,9%), with the beam angles: 0°, 35°,180° and 325°. The gamma pass rate for case 2 were lower than for the other cases, which was due the angular dependence was more prominent for the angle combination 0°-180° (Table 12). The effect of the Delta^4 phantom+ angular dependence was less prominent for the use of more than two beam angles (Figure 21-22). The angular dependence was not a problem for the clinical TH plans (Figure 21-22), because the effect is diluted over the 360° gantry rotation, which make the Delta^4 phantom+ a more suitable tool for QC of TH than TD plans.

The results from the measurement of the lateral target indicated that the Delta^4 phantom+ response was dependent of the target position. These results are consistent with the theory, since in the central area, the diodes are spaced at 5 mm intervals and outside the central area at 10 mm intervals. Hence, the phantom is more sensitive in the central area than peripheral.

In this thesis the gamma pass rate (global) has been used as a tool for patient specific QC, despite the limitations/challenges of the gamma pass rate (27). AAPM TG218 has reported that different computational approaches can produce a significant variability in the calculation of the gamma between different software. For example, the use of global or local dose

normalization and the passing criteria. It has also been reported that IMRT QC evaluation of plans that have large low dose regions cause the fraction of failed points to appear small even when the region of failed points is large compared to the high-dose regions, which result in easily passing gamma test (27).

6.3. Robustness

The results from the motion measurements (Table 13 and Table 14) gave only an indication of the TD robustness, though limited by the measurement of only one paired plan. Regardless of the treatment technique, the results indicated that the tomotherapy system was robust for +5 mm motion in cranio-caudal direction. For larger motion (+20 mm in cranio-caudal), the results dropped below the clinical acceptable threshold. A motion of +20 mm in cranio-caudal direction might seem extreme, but in a study by Feng et al (2009) for pancreas cancer, they reported an amplitude of average tumor motion of 20 mm in cranio-caudal using Cine MRI (28). The results from our study indicated that none of the tomotherapy techniques were suitable for such a large motion.

The comparison of the gamma pass rate between TH and TD plans when introducing simulation motion both in cranio-caudal and anterior-posterior showed that TH was more robust in its delivery. This result may be explained by the fact that TH uses several beams for irradiation, and the effect of the sharp dose gradient perpendicular to the motion was diluted.

In terms of robustness, the advantage of TD is the possibility to use beam expansion for opening additional leaves beyond the target to compensate for the blurring effect caused by target motion. This function is called Flash and is mainly used for breast irradiation. The Flash effect has been studied by Kang D.G et al (2015) for breast irradiation (12). The study showed that for breast irradiation the effect of set-up errors in patient positioning can be reduced by using Flash. In our study, Flash was used for only one case (case 3, Table 1) with the diagnose contralateral axillary involvement in breast cancer recurrence, to compensate for target motion.

7. Summary and conclusions

According to the comparison study of using TD in the thoracic and abdominal region, the benefits of TD relative to TH were reduced beam-on time for some cases (abdominal cases) and a reduced low dose volume (dose bath). In contrast, TH provided better conformity and homogeneity. Compared to 3DCRT, TD provided a significantly higher PTV coverage. This study showed that TD might be an effective radiotherapy technique for several diagnoses in the thoracic and abdominal region.

The present QC method (Delta^4 phantom+) was suitable for measuring TD plans with ≥ 3 beam angles. The angular dependence of the Delta^4 phantom+ might be problematic for measuring TD plans with only two beam angles. The tomotherapy system seemed to be robust for motion amplitude of +5 mm, regardless of the used technique. Further research using simulated motion could bring more clarity about TD robustness in the thoracic and abdominal region.

8. Future work

A modern clinic is required to have multiple treatment alternatives for patient treatment. Over the past years, TD has been implemented in several clinics around the world for breast treatment. In this study, a beginning of an evaluation of TD as a treatment alternative was performed for patients with cancer in the thoracic and abdominal region. Further optimization of TD has to be performed before clinical implementation, for example investigation of the benefits of TD for larger sample size with a specific diagnose. In this study, only 20 cases were used, with different diagnoses.

The limitation (angle dependence) of the present QC method might be a problem for the implementation of TD. Hence, a new QC method should be investigated. Accuray provides a QC method called Delivery Analysis™ for the tomotherapy system. Delivery Analysis uses information from the on-board MVCT detectors in the tomotherapy system to measure differences between expected and delivered MLC performance. Based on the reconstructed MLC delivery pattern, the dose distribution can be calculated for every patient. From exit detector data, an analysis of the exit fluence is generated for every treatment fraction. This is useful to verify if the treatment is delivered as expected to the target (29). This QC method in contrast to the Delta^4 phantom+, should be angle independent and more suitable for TD. As there is no phantom to position on the couch, which takes time from the worker (physicist), Delivery Analysis might also be a more time efficient QC method.

9. Acknowledgements

I would like to thank my supervisors:

Kristoffer Petersson- thank you for always answering my questions and always being close at hand. I appreciate that you spent time to perform measurements with me at the evenings.

Per Engström- thank you for your inputs and feedback. Your ideas and support have been appreciated throughout the work.

I would also like to thank the treatments planners for your tips and tricks with treatment planning.

Last but not least, I would especially like to thank my family and friends for your love and support.

10. References

1. Cancerfonden. Cancerfondsrapporten 2017. 2017;1–137.
2. Bortfeld T, Jiang SB, Rietzel E. Effects of Motion on the Total Dose Distribution. Semin Radiat Oncol. 2004;14(1):41–51.
3. Fredh A, Scherman JB, Fog LS, Munck P. Patient QA systems for rotational radiation therapy : A comparative experimental study with intentional errors. 2013;40(3):1–9.
4. Fraass A. The development of conformal radiation therapy. Med Phys. 1995;22(11):1911–21.
5. Taylor A, Powell MEB. Intensity-modulated radiotherapy - What is it? Cancer Imaging. 2004;4(2):68–73.
6. Podgorsak EB. Radiation Oncology Physics: A Handbook for Teachers and Students. Podgorsak EB, editor. Vienna: IAEA; 2005.
7. Mackie TR, Holmes T, Swerdloff S, Reckwerdt P, Deasy JO, Yang J, et al. Tomotherapy: a new concept for the delivery of conformal radiotherapy. Med Phys. 1993;20(6):1709–19.
8. Jeraj R, Mackie TR, Balog J, Olivera G, Pearson D, Kapatoes J, et al. Radiation characteristics of helical tomotherapy. Med Phys. 2004;31(2):396–404.
9. O'Donnell H, Cooke K, Walsh N, Plowman PN. Early Experience of Tomotherapy-based Intensity-modulated Radiotherapy for Breast Cancer Treatment. Clin Oncol. 2009;21(4):294–301.
10. Petersson K, Gebre-Medhin M, Ceberg C, Nilsson P, Engström P, Knöös T, et al. Haematological toxicity in adult patients receiving craniospinal irradiation - Indication of a dose-bath effect. Radiother Oncol. 2014;111(1):47–51.
11. Schubert LK, Gondi V, Sengbusch E, Westerly DC, Soisson ET, Paliwal BR, et al. Dosimetric comparison of left-sided whole breast irradiation with 3DCRT, forward-planned IMRT, inverse-planned IMRT, helical tomotherapy, and topotherapy. Radiother Oncol. 2011;100(2):241–6.
12. Kang DG, Park SI, Kim SH, Chung MJ, Lee KM, Lee JH. Evaluation of the Flash effect in breast irradiation using TomoDirect: An investigational study. J Radiat Res. 2015;56(2):397–404.
13. Franco P, Zeverino M, Migliaccio F, Sciacero P, Cante D, Borca VC, et al. Intensity-modulated adjuvant whole breast radiation delivered with static angle tomotherapy (TomoDirect): A prospective case series. J Cancer Res Clin Oncol. 2013;139(11):1927–36.
14. Langen KM, Papanikolaou N, Balog J, Crilly R, Followill D, Goddu SM, et al. QA for helical tomotherapy: Report of the AAPM Task Group 148. Med Phys. 2010;37(9):4817–53.
15. Piotrowski T, Skońska M, Jodda A, Ryczkowski A, Kazmierska J, Adamska K, et al. Tomotherapy - A different way of dose delivery in radiotherapy. Wspolczesna Onkol. 2012;16(1):16–25.
16. Fields EC, Rabinovitch R, Ryan NE, Miften M, Westerly DC. A detailed evaluation of TomoDirect 3DCRT planning for whole-breast radiation therapy. Med Dosim. 2013;38(4):401–6.
17. ScandiDos. Delta4 phantom+ [Internet]. Available from: www.scandidos.com
18. Feygelman V, Opp D, Javedan K, Saini AJ, Zhang G. Evaluation of a 3D Diode Array Dosimeter for Helical Tomotherapy Delivery QA. Med Dosim. 2010;35(4):324–9.
19. Knöös T, Kristensen I, Nilsson P. Volumetric and Dosimetric Evaluation of Radiation: radiation conformity index. Int J Radiat Oncol Biol Phys. 1998;42(5):1169–76.
20. Kataria T, Sharma K, Subramani V, Karrthick K, Bisht S. Homogeneity Index: An objective tool for assessment of conformal radiation treatments. J Med Phys. 2012;37(4):207–13.
21. Mould RF. Introductory Medical Statistics. 3rd ed. Mould RF, Orton CG, Spaan JAE, Webster JG, editors. Bristol and Philadelphia: Institute of Physics; 1998.
22. Gibbons JD, Chakraborti S. Nonparametric Statistical Inference. 4th ed. Owen D, Schucany WR, Kshirsagar AM, Neuts MF, Schilling EG, editors. New York: Marcel Dekker; 2003.
23. Marks, Lawrence B, Yorke, Ellen D, Jackson, Andrew, Ten Haken, Randall K, Constine LS, Eisbruch A, Bentzen SM. The use of normal tissue complication probability (NTCP) models in the clinic. Int J Radiat Oncol Biol Phys. 2010;76(3 0):10–9.

24. Gonzalez VJ, Buchholz DJ, Langen KM, Olivera GH, Chauhan B, Meeks SL, et al. Evaluation of two tomotherapy-based techniques for the delivery of whole-breast intensity-modulated radiation therapy. Int J Radiat Oncol Biol Phys. 2006;65(1):284–90.
25. Murai T, Shibamoto Y, Manabe Y, Murata R, Sugie C, Hayashi A, et al. Intensity-modulated radiation therapy using static ports of tomotherapy (TomoDirect): Comparison with the TomoHelical mode. Radiat Oncol. 2013;8(68):1–7.
26. Jones R, Yang W, Read P, Sheng K. Radiation therapy of post-mastectomy patients with positive nodes using fixed beam tomotherapy. Radiother Oncol. 2011;100(2011):247–52.
27. Miften M, Olch A, Mihailidis D, Morean J, Pawlicki T, Molineu A, et al. Tolerance limits and methodologies for IMRT measurement-based verification QA : Recommendations of AAPM Task Group No . 218. Med Phys. 2018;45(4):e53–83.
28. Feng M, Balter JM, Normolle D, Adusumilli S, Cao Y, Chenevert TL, et al. Characterization of Pancreatic Tumor Motion Using Cine MRI: Surrogates for Tumor Position Should Be Used With Caution. Int J Radiat Oncol Biol Phys. 2009;74(3):884–91.
29. Accuray. Delivery Analysis Added Confidence for Every Patient, Every Fraction. 2016.
30. Low D a., Harms WB, Mutic S, Purdy J a. A technique for the quantitative evaluation of dose distributions. Med Phys. 1998;25(5):656–61.
31. Petersson K. Optimising the clinical use of tomotherapy. Lund University; 2014.

Appendix A

Gamma evaluation

The gamma evaluation is a method for comparison of measured and calculated dose distribution (30). The method is based on the use of the measured distribution as the reference information and the calculated is queried for comparison. Two acceptance criteria are used for evaluation, the first is the dose difference ΔD_M and the second is the distance- to agreement Δd_M. A combination of the two criteria are represented by the ellipsoid in Figure A1.

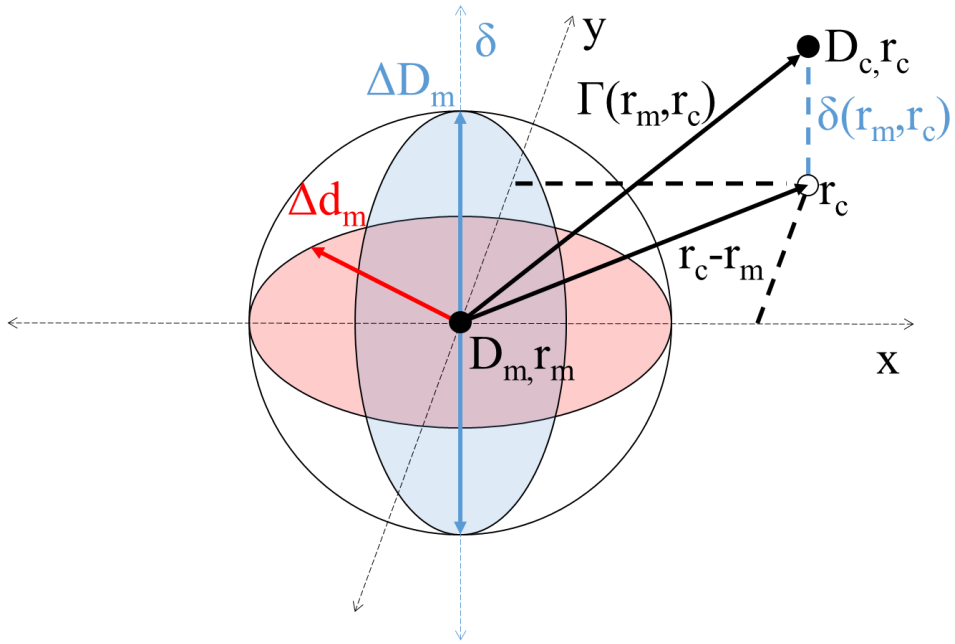

Figure A1. Schematic representation of the combined dose distribution criteria: dose-difference and distance to agreement (31).

In the figure, the measurement point is lying in the origin and denoted with $\mathbf{r}_m$ and the spatial location of the calculated distribution relative to the measured point denoted with $\mathbf{r}_c$**.** The difference between measured dose $[D_m(\mathbf{r}_m)]$ and calculated dose $[D_c(\mathbf{r}_c)]$ is represented by δ. The radius of the disc in the $\mathbf{r}_c - \mathbf{r}_m$ plane is equal to the distance to agreement criteria Δd_M and represented by the pink disc. The dose difference ΔD_M is represented by the blue disc in Figure A1. The surface of the ellipsoid in Figure A1 is mathematically described by Eq. A 1:

$$1 = \sqrt{\frac{r^2(\mathbf{r}_m, \mathbf{r})}{\Delta d_M^2} + \frac{\delta^2(\mathbf{r}_m, \mathbf{r})}{\Delta D_M^2}}, \qquad \textit{Eq. A 1}$$

where

$$r(\mathbf{r}_m, \mathbf{r}) = |\mathbf{r} - \mathbf{r}_m|, \qquad \textit{Eq. A 2}$$

and

$$\delta(\mathbf{r}_m, \mathbf{r}) = D(\mathbf{r}) - D_m(\mathrm{r}_m) \qquad \textit{Eq. A 3}$$

is the dose difference in the position $\mathbf{r}_m$. The combination of the two acceptance criterium are fulfilled at $\mathbf{r}_m$ if any part of $D_c(\mathbf{r}_c)$ surface intersects the ellipsoid defined by Eq. A 1. The γ-index is then calculated by following equation:

$$\gamma(\mathbf{r}_m) = \min\{\Gamma(\mathbf{r}_m, \mathbf{r}_c)\}\forall\{\mathbf{r}_c\} \quad \textit{Eq. A 4}$$

where

$$\Gamma(\mathbf{r}_m, \mathbf{r}_c) = \sqrt{\frac{r^2(\mathbf{r}_m, \mathbf{r}_c)}{\Delta d_M^2} + \frac{\delta^2(\mathbf{r}_m, \mathbf{r}_c)}{\Delta D_M^2}}, \quad \textit{Eq. A 5}$$

$$r(\mathbf{r}_m, \mathbf{r}_c) = |\mathbf{r_c} - \mathbf{r}_m|, \quad \textit{Eq. A 6}$$

and

$$\delta(\mathbf{r}_m, \mathbf{r_c}) = D_c(\mathbf{r}_c) - D_m(\mathbf{r}_m) \quad \textit{Eq. A 7}$$

is the difference between calculated and measured dose distribution. The pass-fails criteria are defined by Eq. A 8.

$$\begin{aligned} \gamma(\mathbf{r}_m) \leq 1, &\quad \text{calculation pass} \\ \gamma(\mathbf{r}_m) > 1, &\quad \text{calculation fails} \end{aligned} \quad \textit{Eq. A 8}$$

Appendix B

PTV Volume

The PTV volume range was 362.8-2449.6 cm^3 for the thoracic cases (Table B1) and 441.4-1511.3 cm^3 for the abdominal cases (Table B2).

Table B1. PTV volume for thoracic cases.

	Case 1	**Case 2**	**Case 3**	**Case 4**	**Case 5**	**Case 6**	**Case 7**	**Case 8**	**Case 9**	**Case 10**
PTV volume [cm^3]	479.6	204.7	424.1	2449.6	858.7	255.0	1224.4	603.0	440.3	362.8

Table B2. PTV volume for abdominal cases.

	Case 1	**Case 2**	**Case 3**	**Case 4**	**Case 5**	**Case 6**	**Case 7**	**Case 8**	**Case 9**	**Case 10**
PTV volume [cm^3]	481.1	1511.3	849.6	484.5	441.4	626.3	551.4	893.4	619.1	1080.7